Water Resources Research

METHOD

10.1029/2024WR039370

An Efficient Quasi-Monte Carlo Method for Concurrent Estimation of First-Order and Total-Effect Process Sensitivity Indices

Jing Yang[1,2,3], Ming Ye[3], Alberto Guadagnini[4,5], Heng Dai[6,7], and Tian Jiao[8]

[1]School of Land Engineering, Chang'an University, Xi'an, China, [2]College of Water Resources and Architectural Engineering, Northwest A&F University, Yangling, China, [3]Department of Earth, Ocean, and Atmosphere Science and Department of Scientific Computing, Florida State University, Tallahassee, FL, USA, [4]Dipartimento di Ingegneria Civile e Ambientale, Politecnico di Milano, Milano, Italy, [5]Sonny Astani Department of Civil and Environmental Engineering, Viterbi School of Engineering, Los Angeles, CA, USA, [6]State Key Laboratory of Geomicrobiology and Environmental Changes, China University of Geosciences, Wuhan, China, [7]Hubei Key Laboratory of Yangtze Catchment Environmental Aquatic Science, China University of Geosciences, Wuhan, China, [8]College of Urban and Environmental Sciences, Northwest University, Xi'an, China

Key Points:

- A quasi-Monte Carlo (MC) method and workflow are rigorously developed for efficiently estimating total-effect process sensitivity index
- The quasi-MC method is employed to concurrently estimate first-order and total-effect process sensitivity indices
- The quasi-MC method converges substantially faster and is more reliable than its traditional brute force MC counterpart

Correspondence to:

M. Ye,
mye@fsu.edu

Citation:

Yang, J., Ye, M., Guadagnini, A., Dai, H., & Jiao, T. (2025). An efficient quasi-Monte Carlo method for concurrent estimation of first-order and total-effect process sensitivity indices. *Water Resources Research*, *61*, e2024WR039370. https://doi.org/10.1029/2024WR039370

Received 4 NOV 2024
Accepted 25 NOV 2025

Abstract Developing and improving process-based models requires identifying the importance and/or influence of various processes driving system behavior. In our recent studies, important processes are identified using first-order process sensitivity index PS_K (Dai et al., 2017, https://doi.org/10.1002/2016wr019715), and non-influential processes are determined using total-effect process sensitivity index PS_{TK} (Yang et al., 2022, https://doi.org/10.1029/2021wr029812), K denoting a given system process. Estimating these indices through the brute force Monte Carlo (MC) method is computationally intensive and often impractical. This study extends the quasi-MC method developed by Dai et al. (2022), https://doi.org/10.1029/2022wr033263 to concurrently estimate PS_K and PS_{TK} with reduced computational cost. The concurrent estimation is based on a rigorous theoretical framework that we leverage to provide a robust computational implementation of the quasi-MC method. The number of model executions required for estimating PS_K or PS_{TK} associated with system process K is reduced from N^2 in brute force MC method to $2N$ in quasi-MC method, N being the number of samples generated for uncertain parameters. The total model executions required to concurrently estimate PS_K and PS_{TK} for all processes of an individual system model are $N \times (N_p + 2)$, N_p being the number of system processes associated with the system model of interest. Convergence, accuracy, and reliability of the quasi-MC method are evaluated through an exemplary one-dimensional groundwater flow example. Results demonstrate that the quasi-MC method converges substantially faster and is more reliable than its brute force MC counterpart. Impacts of process model weights on estimating the two indices and their theoretical and practical limitations are also discussed.

1. Introduction

Development and improvement of process-based models require identifying the importance (in a relative sense) of the processes embedded therein. Processes that are deemed important should be accurately represented, for example, through exhaustive monitoring and data collection campaigns to sharpen our ability for process characterization (Antonetti et al., 2016; Clark et al., 2015; Razavi & Gupta, 2015). Processes that are identified as non-influential to a target model output could be simplified (or even ignored) when resources and/or time are limited (Mai, 2023; Markstrom et al., 2016; Schäfer Rodrigues Silva et al., 2020). Sensitivity analysis methods have been developed to assist the identification of important and non-influential model parameters (e.g., Ceriotti et al., 2018; Dell'Oca et al., 2017; Devak & Dhanya, 2017; Knabe et al., 2021; Li et al., 2021; Markstrom et al., 2016; Nossent et al., 2011; Song et al., 2015; Su & Li, 2022). However, relying on these methods (in general) does not enable one to identify important or non-influential system processes, except under special circumstances where parameter importance/influence is equivalent to process importance/influence (Elshall et al., 2020; Wagena et al., 2019; Yang et al., 2024; Yang & Ye, 2022). Traditional sensitivity analysis methods targeting quantification of uncertain model parameter importance have then been expanded to enable one to rank the relative importance of processes embedded in a model for a given model output. For example, Dai et al. (2017) rely on a variance-based sensitivity analysis method and develop a first-order process sensitivity index (hereafter denoted as PS_K) to identify important processes. Yang et al. (2022) extend the concept of total-effect parameter sensitivity index to

define a total-effect process sensitivity index (hereafter denoted as PS_{TK}) to enable identification of non-influential processes. The method of Dai et al. (2017) is incorporated into a multi-assumption architecture and testbed (Walker et al., 2018). The two process sensitivity indices illustrated above have been used in several recent works (Dai et al., 2022, 2024; Walker et al., 2021; Xu et al., 2019; Yang & Ye, 2022; Yang et al., 2022, 2024; Yu et al., 2024). In this context, our study is focused on key technical aspects associated with the computational burden related to the estimation of the two process sensitivity indices. A distinctive objective of this study is to concurrently estimate the first-order and total-effect process sensitivity indices in a sound and computationally efficient manner.

From the perspective of process-based modeling, a system can be viewed as an integration of multiple processes and their interactions. In the absence of model uncertainty, a physical process is represented by a single process model (or formulation). By integrating the process models of all processes involved, one can construct a unique model that represents the overall system behavior. In the presence of process model uncertainty, a system process may be represented by multiple alternative process models (or formulations). The set of process models one can consider to represent process K is here collected in vector $\mathbf{M}_K(\theta_K) = \{M_{K_1}(\theta_{K_1}), M_{K_2}(\theta_{K_2}), ...\}$, where each process model is associated with its own set of parameters. In this case, process K may be represented by alternative process models M_{K_1}, M_{K_2}, … (here M_{K_1} and M_{K_2} are characterized by parameter(s) θ_{K_1} and θ_{K_2}, respectively). A conceptual framework according to which one can consider diverse process models leads to multiple possible system models that represent the system, $\mathbf{M}(\theta) = \cup(\mathbf{M}_K(\theta_K), \mathbf{M}_S(\theta_S), ...)$, where $\cup$ represents integration of process models of processes K, S, …, into system models. As an example, if the dynamics of a hydrogeological system are governed by two processes (e.g., recharge and geology) and each process can be represented by five alternative process models, then there are a total of 25 system models (Ye et al., 2010). When considering process model uncertainty, the first-order process sensitivity index, PS_K, and the total-effect process sensitivity index, PS_{TK}, are defined as (Dai et al., 2017; Yang et al., 2022):

$$PS_K = \frac{V_{\mathbf{M}_K}\left(E_{\mathbf{M}_{\sim K}}(\Delta|M_K)\right)}{V(\Delta)} = 1 - \frac{E_{\mathbf{M}_K}\left(V_{\mathbf{M}_{\sim K}}(\Delta|M_K)\right)}{V(\Delta)}, \tag{1}$$

$$PS_{TK} = \frac{E_{\mathbf{M}_{\sim K}}\left(V_{\mathbf{M}_K}(\Delta|M_{\sim K})\right)}{V(\Delta)} = 1 - \frac{V_{\mathbf{M}_{\sim K}}\left(E_{\mathbf{M}_K}(\Delta|M_{\sim K})\right)}{V(\Delta)}, \tag{2}$$

Here, Δ denotes a scalar model output; M_K is a process model included in model set $\mathbf{M}_K$ that can be employed to represent process K; and $M_{\sim K}$ is a process model in model set $\mathbf{M}_{\sim K}$ that can be employed to represent all processes except process K (hereinafter referred to as processes $\sim K$). The term $V_{\mathbf{M}_K}\left(E_{\mathbf{M}_{\sim K}}(\Delta|M_K)\right) = V(\Delta) - E_{\mathbf{M}_K}\left(V_{\mathbf{M}_{\sim K}}(\Delta|M_K)\right)$ in Equation 1 measures the average (over all process models associated with process K) variance reduction conditional to identification of the model of process K. A large variance reduction corresponds to an important process. The term $E_{\mathbf{M}_{\sim K}}\left(V_{\mathbf{M}_K}(\Delta|M_{\sim K})\right)$ in Equation 2 measures the average (over all process models associated with processes $\sim K$, i.e., all processes except process K) variance remained if the process models of processes $\sim K$ are deterministically known. A small remaining variance denotes a non-influential process, i.e., a process that is neither important nor interacting with other processes). The mean and variance appearing in Equations 1 and 2 are evaluated over the collection of alternative process models and can be estimated by any model averaging methods (e.g., Ye et al., 2004, 2008).

Estimating these two process sensitivity indices through a typical brute force Monte Carlo (MC) method is conceptually straightforward. It is otherwise computationally expensive when addressing both parameter and model uncertainty. In the presence of parameter uncertainty and relying on the laws of total mean and of total variance, the term $V_{\mathbf{M}_K}\left(E_{\mathbf{M}_{\sim K}}(\Delta|M_K)\right)$ in Equation 1 is expanded as (Dai et al., 2017)

$$\begin{aligned} V_{\mathbf{M}_K}\left(E_{\mathbf{M}_{\sim K}}(\Delta|M_K)\right) = {} & E_{\mathbf{M}_K}E_{\boldsymbol{\theta}_K|M_K}\left(E_{\mathbf{M}_{\sim K}}E_{\boldsymbol{\theta}_{\sim K}|M_{\sim K}}(\Delta|\theta_K, M_K, \theta_{\sim K}, M_{\sim K})\right)^2 \\ & - \left(E_{\mathbf{M}_K}E_{\boldsymbol{\theta}_K|M_K}E_{\mathbf{M}_{\sim K}}E_{\boldsymbol{\theta}_{\sim K}|M_{\sim K}}(\Delta|\theta_K, M_K, \theta_{\sim K}, M_{\sim K})\right)^2. \end{aligned} \tag{3}$$

Here, subscript $\boldsymbol{\theta}_K|M_K$ indicates that the expectation is taken with respect to parameter $\boldsymbol{\theta}_K$, which is considered a random variable associated with process model M_K; subscript $\boldsymbol{\theta}_{\sim K}|M_{\sim K}$ indicates that the expectation is taken with respect to parameter $\boldsymbol{\theta}_{\sim K}$ associated with process model $M_{\sim K}$; and notation $\Delta|\theta_K, M_K, M_{\sim K}, \theta_{\sim K}$ indicates that Δ is a model output stemming from a system model formulation obtained by integrating M_K and $M_{\sim K}$ associated with corresponding parameter realizations θ_K of $\boldsymbol{\theta}_K$ and $\theta_{\sim K}$ of $\boldsymbol{\theta}_{\sim K}$, respectively. We note that the relationship between parameter realization θ_K and random parameter $\boldsymbol{\theta}_K$ corresponds to the relationship between a realization x and the random variable X from which x is sampled (as typically denoted in standard statistical textbooks). This also applies to the relationship between parameter realization $\theta_{\sim K}$ and random parameter $\boldsymbol{\theta}_{\sim K}$. Similar to Equation 3, $V_{\mathbf{M}_{\sim K}}\left(E_{\mathbf{M}_K}\left(\Delta|M_{\sim K}\right)\right)$ of Equation 2 is expanded as (Yang et al., 2022)

$$\begin{aligned} V_{\mathbf{M}_{\sim K}}\left(E_{\mathbf{M}_K}\left(\Delta|M_{\sim K}\right)\right) = {} & E_{\mathbf{M}_{\sim K}} E_{\boldsymbol{\theta}_{\sim K}|M_{\sim K}}\left(E_{\mathbf{M}_K} E_{\boldsymbol{\theta}_K|M_K}\left(\Delta|\theta_K, M_K, \theta_{\sim K}, M_{\sim K}\right)\right)^2 \\ & - \left(E_{\mathbf{M}_{\sim K}} E_{\boldsymbol{\theta}_{\sim K}|M_{\sim K}} E_{\mathbf{M}_K} E_{\boldsymbol{\theta}_K|M_K}\left(\Delta|\theta_K, M_K, \theta_{\sim K}, M_{\sim K}\right)\right)^2, \end{aligned} \tag{4}$$

to address both process model and parameter uncertainties.

As illustrated in Dai et al. (2017) and Yang et al. (2022), numerical estimation of Equations 3 and 4 requires four nested loops. These are performed over: (a) the set of process models $\mathbf{M}_K$, (b) the set of parameter realizations, $\boldsymbol{\theta}_K$, associated with process model M_K in model set $\mathbf{M}_K$, (c) the set of process models $\mathbf{M}_{\sim K}$, and (d) the set of parameter realizations, $\boldsymbol{\theta}_{\sim K}$, associated with process model $M_{\sim K}$ in model set $\mathbf{M}_{\sim K}$. Because of the four nested loops, evaluating Equations 3 or 4 using a brute force MC method requires a total of $(m_K \times n_K) \times (m_{\sim K} \times n_{\sim K})$ (or equivalently, $(m_{\sim K} \times n_{\sim K}) \times (m_K \times n_K)$) model executions. Here, m_K and $m_{\sim K}$ denote the number of alternative process models in $\mathbf{M}_K$ and $\mathbf{M}_{\sim K}$, respectively; and n_K and $n_{\sim K}$ are the number of parameter realizations in $\boldsymbol{\theta}_K$ and $\boldsymbol{\theta}_{\sim K}$, respectively. By way of example, considering $n_K = n_{\sim K} = N$ leads to a number of brute force MC simulations equal to $m_K \times m_{\sim K} \times N^2$. The latter can be in the order of magnitude of millions, for example, for $N = 1{,}000$. Dai et al. (2022) reduce the number of MC simulations from $m_K \times m_{\sim K} \times N^2$ to $m_K \times m_{\sim K} \times 2N$. They do so by developing a quasi-MC method (Saltelli et al., 2010) that removes the four nested loops upon relying on three sets of parameter samples. These authors only tackle estimation of the first-order process sensitivity index, PS_K, of process K.

This study expands the quasi-MC method of Dai et al. (2022) to concurrently, rather than separately, estimate the first-order and total-effect process sensitivity indices for a system process, hence aiming at further reducing computational cost. Such a concurrent estimation is theoretically possible due to the similarities between Equations 3 and 4. As detailed in Section 2.3, when developing computer codes for concurrently estimating the two indices, the expressions of the quasi-MC method developed for these indices are simplified by using three matrices of parameter samples. The ensuing simplified expressions rest on the computational method of Saltelli et al. (2010) for concurrently estimating the first-order and total-effect parameter sensitivity indices of a single system model. It should be noted that our method is not a straightforward application of the method of Saltelli et al. (2010) to multiple system models. Instead, we re-design the sample matrices to account for the possibility of employing multiple system models to concurrently estimate PS_K and PS_{TK} for all processes. Estimation of the two process sensitivity indices for each system process requires a total number of MC simulations equal to $(m_k \times m_{\sim k}) \times N \times (N_p + 2)$, where N_p is the number of processes. Derivation of the associated simplified expressions and their computational implementation constitute a unique contribution of our study to process sensitivity analysis. The new quasi-MC method is evaluated by applying it to groundwater flow modeling for estimating the two process sensitivity indices associated with three groundwater processes.

2. Methodology

2.1. Use of Three Sets of Parameter Samples for Efficient Estimation of PS_{TK}

Following Dai et al. (2022), we provide the mathematical derivation for the efficient estimation of the total-effect process sensitivity index, PS_{TK}, by removing the two nested parameter loops upon relying on three sets of

parameter samples. The first term $E_{\mathbf{M}_{\sim K}}E_{\boldsymbol{\theta}_{\sim K}|M_{\sim K}}\left(E_{\mathbf{M}_K}E_{\boldsymbol{\theta}_K|M_K}\left(\Delta|\theta_K,M_K,\theta_{\sim K},M_{\sim K}\right)\right)^2$ in the right-hand side of Equation 4 is expanded as:

$$
\begin{aligned}
&E_{\mathbf{M}_{\sim K}}E_{\boldsymbol{\theta}_{\sim K}|M_{\sim K}}\left(E_{\mathbf{M}_K}E_{\boldsymbol{\theta}_K|M_K}\left(\Delta|\theta_K,M_K,\theta_{\sim K},M_{\sim K}\right)\right)^2\\
&= E_{\mathbf{M}_{\sim K}}E_{\boldsymbol{\theta}_{\sim K}|M_{\sim K}}\left(\begin{array}{l}\sum_{p=1}^{m_K}\left(E_{\boldsymbol{\theta}_{K_p}|M_{K_p}}\left(\Delta|\theta_{K_p},M_{K_p},\theta_{\sim K},M_{\sim K}\right)\right)^2P(M_{K_p})^2\\ +\sum_{p=1}^{m_K}\sum_{\substack{r=1\\r\neq p}}^{m_K}\left(\begin{array}{l}E_{\boldsymbol{\theta}_{K_p}|M_{K_p}}\left(\Delta|\theta_{K_p},M_{K_p},\theta_{\sim K},M_{\sim K}\right)\\ \times E_{\boldsymbol{\theta}_{K_r}|M_{K_r}}\left(\Delta|\theta_{K_r},M_{K_r},\theta_{\sim K},M_{\sim K}\right)\end{array}\right)P(M_{K_p})P(M_{K_r})\end{array}\right)\\
&= \sum_{q=1}^{m_{\sim K}}E_{\boldsymbol{\theta}_{\sim K_q}|M_{\sim K_q}}\left(\begin{array}{l}\sum_{p=1}^{m_K}\left(E_{\boldsymbol{\theta}_{K_p}|M_{K_p}}\left(\Delta|\theta_{K_p},M_{K_p},\theta_{\sim K_q},M_{\sim K_q}\right)\right)^2P(M_{K_p})^2\\ +\sum_{p=1}^{m_K}\sum_{\substack{r=1\\r\neq p}}^{m_K}\left(\begin{array}{l}E_{\boldsymbol{\theta}_{K_p}|M_{K_p}}\left(\Delta|\theta_{K_p},M_{K_p},\theta_{\sim K_q},M_{\sim K_q}\right)\\ \times E_{\boldsymbol{\theta}_{K_r}|M_{K_r}}\left(\Delta|\theta_{K_r},M_{K_r},\theta_{\sim K_q},M_{\sim K_q}\right)\end{array}\right)P(M_{K_p})P(M_{K_r})\end{array}\right)P\left(M_{\sim K_q}\right)\\
&= \sum_{q=1}^{m_{\sim K}}\sum_{p=1}^{m_K}E_{\boldsymbol{\theta}_{\sim K_q}|M_{\sim K_q}}\left(E_{\boldsymbol{\theta}_{K_p}|M_{K_p}}\left(\Delta|\theta_{K_p},M_{K_p},\theta_{\sim K_q},M_{\sim K_q}\right)\right)^2P(M_{K_p})^2P\left(M_{\sim K_q}\right)\\
&+\sum_{q=1}^{m_{\sim K}}\sum_{p=1}^{m_K}\sum_{\substack{r=1\\r\neq p}}^{m_K}E_{\boldsymbol{\theta}_{\sim K_q}|M_{\sim K_q}}\left(\begin{array}{l}E_{\boldsymbol{\theta}_{K_p}|M_{K_p}}\left(\Delta|\theta_{K_p},M_{K_p},\theta_{\sim K_q},M_{\sim K_q}\right)\\ \times E_{\boldsymbol{\theta}_{K_r}|M_{K_r}}\left(\Delta|\theta_{K_r},M_{K_r},\theta_{\sim K_q},M_{\sim K_q}\right)\end{array}\right)P(M_{K_p})P(M_{K_r})P\left(M_{\sim K_q}\right)
\end{aligned}
\quad , \tag{5}
$$

Here, $q = 1, 2, \ldots, m_{\sim K}$ is the index associated with process models for all processes except for process K; $p = 1, 2, \ldots, m_K$ and $r = 1, 2, \ldots, m_K$ $(r \neq p)$ are the indices associated with process models for process K. Subscript $\boldsymbol{\theta}_{\sim K_q}|M_{\sim K_q}$ of $E_{\boldsymbol{\theta}_{\sim K_q}|M_{\sim K_q}}$ indicates that the expectation is taken with respect to the qth process model $M_{\sim K_q}$, that is, considered to represent all processes except for process K. Similarly, subscripts $\boldsymbol{\theta}_{K_p}|M_{K_p}$ of $E_{\boldsymbol{\theta}_{K_p}|M_{K_p}}$ and $\boldsymbol{\theta}_{K_r}|M_{K_r}$ of $E_{\boldsymbol{\theta}_{K_r}|M_{K_r}}$ indicate that these expectations are taken with respect to the p-th and the r-th process models M_{K_p} and M_{K_r}, respectively, that represent process K. Quantities $P\left(M_{\sim K_q}\right)$, $P(M_{K_p})$, and $P(M_{K_r})$ denote the weights of process models $M_{\sim K_q}$, M_{K_p}, and M_{K_r}, respectively, and are used for model averaging. Expressing the term $E_{\boldsymbol{\theta}_{\sim K_q}|M_{\sim K_q}}\left(E_{\boldsymbol{\theta}_{K_p}|M_{K_p}}\left(\Delta|\theta_{K_p},M_{K_p},\theta_{\sim K_q},M_{\sim K_q}\right)\right)^2$ appearing on the right-hand side of Equation 5 into an integral form yields:

$$
\begin{aligned}
&E_{\boldsymbol{\theta}_{\sim K_q}|M_{\sim K_q}}\left(E_{\boldsymbol{\theta}_{K_p}|M_{K_p}}\left(\Delta|\theta_{K_p},M_{K_p},\theta_{\sim K_q},M_{\sim K_q}\right)\right)^2\\
&= \int_{\boldsymbol{\theta}_{\sim K_q}}\left(E_{\boldsymbol{\theta}_{K_p}|M_{K_p}}\left(\Delta|\theta_{K_p},M_{K_p},\theta_{\sim K_q},M_{\sim K_q}\right)\right)^2p\left(\theta_{\sim K_q}|M_{\sim K_q}\right)d\theta_{\sim K_q}
\end{aligned}
\quad , \tag{6}
$$

where $p\left(\theta_{\sim K_q}|M_{\sim K_q}\right)$ is the probability density function (PDF) of $\theta_{\sim K_q}$ associated with process model $M_{\sim K_q}$. Following Saltelli et al. (2010), we recast $\left(E_{\boldsymbol{\theta}_{K_p}|M_{K_p}}\left(\Delta|\theta_{K_p},M_{K_p},\theta_{\sim K_q},M_{\sim K_q}\right)\right)^2$ in Equation 6 into a corresponding integral form as:

$$\begin{aligned}
&\left(E_{\boldsymbol{\theta}_{K_p}|M_{K_p}}\left(\Delta|\theta_{K_p},M_{K_p},\theta_{\sim K_q},M_{\sim K_q}\right)\right)^2\\
&=\left(E_{\boldsymbol{\theta}_{K_p}|M_{K_p}}\left(\Delta|\theta_{K_p},M_{K_p},\theta_{\sim K_q},M_{\sim K_q}\right)\right)\left(E_{\boldsymbol{\theta}_{K_p}|_{M_{K_p}}}\left(\Delta|\theta_{K_p},M_{K_p},\theta_{\sim K_q},M_{\sim K_q}\right)\right)\\
&=\iint_{\boldsymbol{\theta}_{K_p},\boldsymbol{\theta}_{K_p}'}\begin{pmatrix}\left(\Delta|\theta_{K_p},M_{K_p},\theta_{\sim K_q},M_{\sim K_q}\right)\left(\Delta|\theta_{K_p}',M_{K_p},\theta_{\sim K_q},M_{\sim K_q}\right)\\ \times\left(p(\theta_{K_p}|M_{K_p})\,d\theta_{K_p}\right)\left(p(\theta_{K_p}'|M_{K_p})\,d\theta_{K_p}'\right)\end{pmatrix}
\end{aligned},\tag{7}$$

where $p(\theta_{K_p}|M_{K_p})$ and $p(\theta_{K_p}'|M_{K_p})$ are the PDFs of parameter θ_{K_p} and θ_{K_p}', respectively, associated with process model M_{K_p}. The double integral in Equation 7 is related to parameter sets $\boldsymbol{\theta}_{K_p}$ and $\boldsymbol{\theta}_{K_p}'$. Here, integration is performed across the support of the PDFs $p(\theta_{K_p}|M_{K_p}) = p(\theta_{K_p}'|M_{K_p})$. Substituting Equation 7 into Equation 6 leads to:

$$\begin{aligned}
&E_{\boldsymbol{\theta}_{\sim K_q}|M_{\sim K_q}}\left(E_{\boldsymbol{\theta}_{K_p}|M_{K_p}}\left(\Delta|\theta_{K_p},M_{K_p},\theta_{\sim K_q},M_{\sim K_q}\right)\right)^2\\
&=\int_{\boldsymbol{\theta}_{\sim K_q}}\left(\iint_{\boldsymbol{\theta}_{K_p},\boldsymbol{\theta}_{K_p}'}\begin{pmatrix}\left(\Delta|\theta_{K_p},M_{K_p},\theta_{\sim K_q},M_{\sim K_q}\right)\left(\Delta|\theta_{K_p}',M_{K_p},\theta_{\sim K_q},M_{\sim K_q}\right)\\ \times\left(p(\theta_{K_p}|M_{K_p})\,d\theta_{K_p}\right)\left(p(\theta_{K_p}'|M_{K_p})\,d\theta_{K_p}'\right)\end{pmatrix}\right)p\left(\theta_{\sim K_q}|M_{\sim K_q}\right)d\theta_{\sim K_q}\\
&=\iiint_{\boldsymbol{\theta}_{\sim K_q},\boldsymbol{\theta}_{K_p},\boldsymbol{\theta}_{K_p}'}\begin{matrix}\left(\Delta|\theta_{K_p},M_{K_p},\theta_{\sim K_q},M_{\sim K_q}\right)\left(\Delta|\theta_{K_p}',M_{K_p},\theta_{\sim K_q},M_{\sim K_q}\right)\\ \times\left(p(\theta_{K_p}|M_{K_p})\,d\theta_{K_p}\right)\left(p(\theta_{K_p}'|M_{K_p})\,d\theta_{K_p}'\right)\left(p\left(\theta_{\sim K_q}|M_{\sim K_q}\right)d\theta_{\sim K_q}\right)\end{matrix}
\end{aligned},\tag{8}$$

where the triple integral in Equation 8 is related to the support of parameters $\boldsymbol{\theta}_{\sim K_q}$, $\boldsymbol{\theta}_{K_p}$, and $\boldsymbol{\theta}_{K_p}'$, respectively associated with PDFs $p\left(\theta_{\sim K_q}|M_{\sim K_q}\right)$, $p(\theta_{K_p}|M_{K_p})$, and $p(\theta_{K_p}'|M_{K_p})$. By virtue of Equation 8, term $E_{\boldsymbol{\theta}_{\sim K_q}|M_{\sim K_q}}\left(E_{\boldsymbol{\theta}_{K_p}|M_{K_p}}\left(\Delta|\theta_{K_p},M_{K_p},\theta_{\sim K_q},M_{\sim K_q}\right)\right)^2$ becomes:

$$\begin{aligned}
&E_{\boldsymbol{\theta}_{\sim K_q}|M_{\sim K_q}}\left(E_{\boldsymbol{\theta}_{K_p}|_{M_{K_p}}}\left(\Delta|\theta_{K_p},M_{K_p},\theta_{\sim K_q},M_{\sim K_q}\right)\right)^2\\
&=E_{\boldsymbol{\theta}_{\sim K_q},\boldsymbol{\theta}_{K_p},\boldsymbol{\theta}_{K_p}'}\left(\left(\Delta|\theta_{K_p},M_{K_p},\theta_{\sim K_q},M_{\sim K_q}\right)\left(\Delta|\theta_{K_p}',M_{K_p},\theta_{\sim K_q},M_{\sim K_q}\right)\right)
\end{aligned}.\tag{9}$$

Applying the same procedure to the second term at the right-hand side of Equation 5 leads to:

$$\begin{aligned}
&E_{\boldsymbol{\theta}_{\sim K_q}|M_{\sim K_q}}\begin{pmatrix}E_{\boldsymbol{\theta}_{K_p}|M_{K_p}}\left(\Delta|\theta_{K_p},M_{K_p},\theta_{\sim K_q},M_{\sim K_q}\right)\\ \times E_{\boldsymbol{\theta}_{K_r}|_{M_{K_r}}}\left(\Delta|\theta_{K_r},M_{K_r},\theta_{\sim K_q},M_{\sim K_q}\right)\end{pmatrix}\\
&=\int_{\boldsymbol{\theta}_{\sim K_q}}\begin{pmatrix}\int_{\boldsymbol{\theta}_{K_p}}\left(\Delta|\theta_{K_p},M_{K_p},\theta_{\sim K_q},M_{\sim K_q}\right)p(\theta_{K_p}|M_{K_p})\,d\theta_{K_p}\\ \times\int_{\boldsymbol{\theta}_{K_r}}\left(\Delta|\theta_{K_r},M_{K_r},\theta_{\sim K_q},M_{\sim K_q}\right)p(\theta_{K_r}|M_{K_r})\,d\theta_{K_r}\end{pmatrix}p\left(\theta_{\sim K_q}|M_{\sim K_q}\right)d\theta_{\sim K_q}\\
&=\int_{\boldsymbol{\theta}_{\sim K_q}}\left(\iint_{\boldsymbol{\theta}_{K_p},\boldsymbol{\theta}_{K_r}}\begin{pmatrix}\left(\Delta|\theta_{K_p},M_{K_p},\theta_{\sim K_q},M_{\sim K_q}\right)\left(\Delta|\theta_{K_r},M_{K_r},\theta_{\sim K_q},M_{\sim K_q}\right)\\ \times\left(p(\theta_{K_p}|M_{K_p})\,d\theta_{K_p}\right)\left(p(\theta_{K_r}|M_{K_r})\,d\theta_{K_r}\right)\end{pmatrix}\right)p\left(\theta_{\sim K_q}|M_{\sim K_q}\right)d\theta_{\sim K_q}\\
&=\iiint_{\boldsymbol{\theta}_{\sim K_q},\boldsymbol{\theta}_{K_p},\boldsymbol{\theta}_{K_r}}\begin{pmatrix}\left(\Delta|\theta_{K_p},M_{K_p},\theta_{\sim K_q},M_{\sim K_q}\right)\left(\Delta|\theta_{K_r},M_{K_r},\theta_{\sim K_q},M_{\sim K_q}\right)\\ \times\left(p(\theta_{K_p}|M_{K_p})\,d\theta_{K_p}\right)\left(p(\theta_{K_r}|M_{K_r})\,d\theta_{K_r}\right)\left(p\left(\theta_{\sim K_q}|M_{\sim K_q}\right)d\theta_{\sim K_q}\right)\end{pmatrix}\\
&=E_{\boldsymbol{\theta}_{\sim K_q},\boldsymbol{\theta}_{K_p},\boldsymbol{\theta}_{K_r}}\left(\left(\Delta|\theta_{K_p},M_{K_p},\theta_{\sim K_q},M_{\sim K_q}\right)\left(\Delta|\theta_{K_r},M_{K_r},\theta_{\sim K_q},M_{\sim K_q}\right)\right)
\end{aligned}.\tag{10}$$

Equations 9 and 10 are the foundation of the quasi-MC method for estimating PS_{TK}. Relying on these enables one to remove the two nested expectations upon reducing these into a single expectation with respect to $\{\boldsymbol{\theta}_{\sim K_q}, \boldsymbol{\theta}_{K_p}, \boldsymbol{\theta}_{K_p}{}'\}$ and $\{\boldsymbol{\theta}_{\sim K_q}, \boldsymbol{\theta}_{K_p}, \boldsymbol{\theta}_{K_r}\}$. Considering Equation 10 as an example, the nested expectation $E_{\boldsymbol{\theta}_{\sim K_q}|M_{\sim K_q}}\left(E_{\boldsymbol{\theta}_{K_p}|M_{Kp}}\left(\Delta|\theta_{K_p}, M_{K_p}, \theta_{\sim K_q}, M_{\sim K_q}\right) \times E_{\boldsymbol{\theta}_{K_r}|M_{K_r}}\left(\Delta|\theta_{K_r}, M_{K_r}, \theta_{\sim K_q}, M_{\sim K_q}\right)\right)$ is reduced to a single expectation $E_{\boldsymbol{\theta}_{\sim K_q}, \boldsymbol{\theta}_{K_p}, \boldsymbol{\theta}_{K_r}}\left(\left(\Delta|\theta_{K_p}, M_{K_p}, \theta_{\sim K_q}, M_{\sim K_q}\right)\left(\Delta|\theta_{K_r}, M_{K_r}, \theta_{\sim K_q}, M_{\sim K_q}\right)\right)$. With reference to the expectations with respect to the sets of parameter samples $\{\boldsymbol{\theta}_{\sim K_q}, \boldsymbol{\theta}_{K_p}, \boldsymbol{\theta}_{K_p}{}'\}$ and $\{\boldsymbol{\theta}_{\sim K_q}, \boldsymbol{\theta}_{K_p}, \boldsymbol{\theta}_{K_r}\}$, we note that the parameter samples can be generated independently, rather than in the two nested loops, as discussed in the following.

2.2. Quasi-MC Method for Estimation of PS_{TK}

Following Dai et al. (2022), expectations in Equations 9 and 10 are evaluated through a quasi-MC method as:

$$\begin{aligned} &E_{\boldsymbol{\theta}_{\sim K_q}|M_{\sim K_q}}\left(E_{\boldsymbol{\theta}_{K_p}|M_{K_p}}\left(\Delta|\theta_{K_p}, M_{K_p}, \theta_{\sim K_q}, M_{\sim K_q}\right)\right)^2 \\ &\approx \frac{1}{N}\sum_{j=1}^{N}\left(\Delta|\theta_{K_p}^{(j)}, M_{K_p}, \theta_{\sim K_q}^{(j)}, M_{\sim K_q}\right)\left(\Delta|\theta_{K_p}^{(j)\prime}, M_{K_p}, \theta_{\sim K_q}^{(j)}, M_{\sim K_q}\right) \end{aligned}, \tag{11}$$

and

$$\begin{aligned} &E_{\boldsymbol{\theta}_{\sim K_q}|M_{\sim K_q}}\begin{pmatrix} E_{\boldsymbol{\theta}_{K_p}|M_{Kp}}\left(\Delta|\theta_{K_p}, M_{K_p}, \theta_{\sim K_q}, M_{\sim K_q}\right) \\ \times E_{\boldsymbol{\theta}_{K_r}|M_{K_r}}\left(\Delta|\theta_{K_r}, M_{K_r}, \theta_{\sim K_q}, M_{\sim K_q}\right) \end{pmatrix} \\ &\approx \frac{1}{N}\sum_{j=1}^{N}\left(\Delta|\theta_{K_p}^{(j)}, M_{K_p}, \theta_{\sim K_q}^{(j)}, M_{\sim K_q}\right)\left(\Delta|\theta_{K_r}^{(j)}, M_{K_r}, \theta_{\sim K_q}^{(j)}, M_{\sim K_q}\right) \end{aligned}. \tag{12}$$

Here, N is the number of randomly generated parameter realizations of $\{\boldsymbol{\theta}_{\sim K_q}, \boldsymbol{\theta}_{K_p}, \boldsymbol{\theta}_{K_p}{}'\}$ and $\{\boldsymbol{\theta}_{\sim K_q}, \boldsymbol{\theta}_{K_p}, \boldsymbol{\theta}_{K_r}\}$, $j = 1, 2, \ldots, N$ denoting the jth parameter realization. The symbol "≈" is used because the Monte Carlo (and quasi-Monte Carlo) estimators provide finite-sample approximations to the true mathematical expectations. Substituting Equations 11 and 12 into Equation 5 yields:

$$\begin{aligned} &E_{\mathbf{M}_{\sim K}}E_{\boldsymbol{\theta}_{\sim K}|M_{\sim K}}\left(E_{\mathbf{M}_K}E_{\boldsymbol{\theta}_K|M_K}\left(\Delta|\theta_K, M_K, \theta_{\sim K}, M_{\sim K}\right)\right)^2 \\ &\approx \sum_{q=1}^{m_{\sim K}}\sum_{p=1}^{m_K}\frac{1}{N}\sum_{j=1}^{N}\left(\Delta|\theta_{K_p}^{(j)}, M_{K_p}, \theta_{\sim K_q}^{(j)}, M_{\sim K_q}\right)\left(\Delta|\theta_{K_p}^{(j)\prime}, M_{K_p}, \theta_{\sim K_q}^{(j)}, M_{\sim K_q}\right)P(M_{K_p})^2P\left(M_{\sim K_q}\right) \\ &+ \sum_{q=1}^{m_{\sim K}}\sum_{p=1}^{m_K}\sum_{\substack{r=1 \\ r\neq p}}^{m_K}\frac{1}{N}\sum_{j=1}^{N}\left(\Delta|\theta_{K_p}^{(j)}, M_{K_p}, \theta_{\sim K_q}^{(j)}, M_{\sim K_q}\right)\left(\Delta|\theta_{K_r}^{(j)}, M_{K_r}, \theta_{\sim K_q}^{(j)}, M_{\sim K_q}\right)P(M_{K_r})P(M_{K_p})P\left(M_{\sim K_q}\right) \end{aligned}. \tag{13}$$

We note that the second term $\left(E_{\mathbf{M}_{\sim K}}E_{\boldsymbol{\theta}_{\sim K}|M_{\sim K}}E_{\mathbf{M}_K}E_{\boldsymbol{\theta}_K|M_K}\left(\Delta|\theta_K, M_K, \theta_{\sim K}, M_{\sim K}\right)\right)^2$ at the right-hand side of Equation 4 corresponds to the square of the total mean, that is, $(E(\Delta))^2$ (Yang et al., 2022). It is evaluated via:

$$\begin{aligned} &(E(\Delta))^2 \\ &= \left(E_{\mathbf{M}_{\sim K}}E_{\boldsymbol{\theta}_{\sim K}|M_{\sim K}}E_{\mathbf{M}_K}E_{\boldsymbol{\theta}_K|M_K}\left(\Delta|\theta_K, M_K, \theta_{\sim K}, M_{\sim K}\right)\right)^2 \\ &\approx \left(\sum_{q=1}^{m_{\sim K}}\sum_{p=1}^{m_K}\frac{1}{N}\sum_{j=1}^{N}\left(\Delta|\theta_{K_p}^{(j)}, M_{K_p}, \theta_{\sim K_q}^{(j)}, M_{\sim K_q}\right)P(M_{K_p})P\left(M_{\sim K_q}\right)\right)^2 \end{aligned}. \tag{14}$$

Finally, substituting Equations 13 and 14 into Equation 4 yields:

Loop [1] over $m_{\sim K}$ process models $M_{\sim K}$ of process $\sim K$ in $\mathbf{M}_{\sim K}$

Loop [2] over m_K process models M_K of process K in $\mathbf{M}_K$

Loop [3] over N parameter realizations $\theta_{\sim K_q}$ of $M_{\sim K_q}$, θ_{K_p} of M_{K_p}, and $\theta_{K_p}{}'$ of M_{K_p}

Compute $\Delta|\theta_{K_p}, M_{K_p}, \theta_{\sim K_q}, M_{\sim K_q}$ and $\Delta|\theta_{K_p}{}', M_{K_p}, \theta_{\sim K_q}, M_{\sim K_q}$

End Loop [3]

Compute $\frac{1}{N}\sum_{j=1}^{N}\left(\Delta|\theta_{K_p}^{(j)}, M_{K_p}, \theta_{\sim K_q}^{(j)}, M_{\sim K_q}\right)\left(\Delta|\theta_{K_p}^{(j)}{}', M_{K_p}, \theta_{\sim K_q}^{(j)}, M_{\sim K_q}\right)$,

$\frac{1}{N}\sum_{j=1}^{N}\left(\Delta|\theta_{K_p}^{(j)}, M_{K_p}, \theta_{\sim K_q}^{(j)}, M_{\sim K_q}\right)\left(\Delta|\theta_{K_r}^{(j)}, M_{K_r}, \theta_{\sim K_q}^{(j)}, M_{\sim K_q}\right)$, and

$\frac{1}{N}\sum_{j=1}^{N}\left(\Delta|\theta_{K_p}^{(j)}, M_{K_p}, \theta_{\sim K_q}^{(j)}, M_{\sim K_q}\right)$

End Loop [2]

Compute $\sum_{p=1}^{m_K}\frac{1}{N}\sum_{j=1}^{N}\left(\Delta|\theta_{K_p}^{(j)}, M_{K_p}, \theta_{\sim K_q}^{(j)}, M_{\sim K_q}\right)\left(\Delta|\theta_{K_p}^{(j)}{}', M_{K_p}, \theta_{\sim K_q}^{(j)}, M_{\sim K_q}\right)P(M_{K_p})^2$,

$\sum_{p=1}^{m_K}\sum_{\substack{r=1\\ r\neq p}}^{m_K}\frac{1}{N}\sum_{j=1}^{N}\left(\Delta|\theta_{K_p}^{(j)}, M_{K_p}, \theta_{\sim K_q}^{(j)}, M_{\sim K_q}\right)\left(\Delta|\theta_{K_r}^{(j)}, M_{K_r}, \theta_{\sim K_q}^{(j)}, M_{\sim K_q}\right)P(M_{K_r})P(M_{K_p})$, and

$\sum_{p=1}^{m_K}\frac{1}{N}\sum_{j=1}^{N}\left(\Delta|\theta_{K_p}^{(j)}, M_{K_p}, \theta_{\sim K_q}^{(j)}, M_{\sim K_q}\right)P\left(M_{K_p}\right)$

End Loop [1]

Compute $\sum_{q=1}^{m_{\sim K}}\sum_{p=1}^{m_K}\frac{1}{N}\sum_{j=1}^{N}\left(\Delta|\theta_{K_p}^{(j)}, M_{K_p}, \theta_{\sim K_q}^{(j)}, M_{\sim K_q}\right)\left(\Delta|\theta_{K_p}^{(j)}{}', M_{K_p}, \theta_{\sim K_q}^{(j)}, M_{\sim K_q}\right)P(M_{K_p})^2P(M_{\sim K_q})$,

$\sum_{q=1}^{m_{\sim K}}\sum_{p=1}^{m_K}\sum_{\substack{r=1\\ r\neq p}}^{m_K}\frac{1}{N}\sum_{j=1}^{N}\left(\Delta|\theta_{K_p}^{(j)}, M_{K_p}, \theta_{\sim K_q}^{(j)}, M_{\sim K_q}\right)\left(\Delta|\theta_{K_r}^{(j)}, M_{K_r}, \theta_{\sim K_q}^{(j)}, M_{\sim K_q}\right)P(M_{K_r})P(M_{K_p})P(M_{\sim K_q})$, and

$\left(\sum_{q=1}^{m_{\sim K}}\sum_{p=1}^{m_K}\frac{1}{N}\sum_{j=1}^{N}\left(\Delta|\theta_{K_p}^{(j)}, M_{K_p}, \theta_{\sim K_q}^{(j)}, M_{\sim K_q}\right)P\left(M_{K_p}\right)P\left(M_{\sim K_q}\right)\right)^2$

Figure 1. Pseudo code implemented in a quasi-MC framework to estimate PS_{TK} through Equation 15. For the computation after Loop [3], subscripts r and p of $\Delta|\theta_{K_r}^{(j)}, M_{K_r}, \theta_{\sim K_q}^{(j)}, M_{\sim K_q}$ and $\Delta|\theta_{K_p}^{(j)}, M_{K_p}, \theta_{\sim K_q}^{(j)}, M_{\sim K_q}$ denote different realizations of model M_K (of process K) and its model parameters θ_K.

$$
\begin{aligned}
&V_{\mathbf{M}_{\sim K}}\left(E_{\mathbf{M}_K}(\Delta|M_{\sim K})\right)\\
&\approx \sum_{q=1}^{m_{\sim K}}\sum_{p=1}^{m_K}\frac{1}{N}\sum_{j=1}^{N}\left(\Delta|\theta_{K_p}^{(j)}, M_{K_p}, \theta_{\sim K_q}^{(j)}, M_{\sim K_q}\right)\left(\Delta|\theta_{K_p}^{(j)}{}', M_{K_p}, \theta_{\sim K_q}^{(j)}, M_{\sim K_q}\right)P(M_{K_p})^2P\left(M_{\sim K_q}\right)\\
&+\sum_{q=1}^{m_{\sim K}}\sum_{p=1}^{m_K}\sum_{\substack{r=1\\ r\neq p}}^{m_K}\frac{1}{N}\sum_{j=1}^{N}\left(\Delta|\theta_{K_p}^{(j)}, M_{K_p}, \theta_{\sim K_q}^{(j)}, M_{\sim K_q}\right)\left(\Delta|\theta_{K_r}^{(j)}, M_{K_r}, \theta_{\sim K_q}^{(j)}, M_{\sim K_q}\right)P(M_{K_r})P(M_{K_p})P\left(M_{\sim K_q}\right).\\
&-\left(\sum_{q=1}^{m_{\sim K}}\sum_{p=1}^{m_K}\frac{1}{N}\sum_{j=1}^{N}\left(\Delta|\theta_{K_p}^{(j)}, M_{K_p}, \theta_{\sim K_q}^{(j)}, M_{\sim K_q}\right)P(M_{K_p})P\left(M_{\sim K_q}\right)\right)^2
\end{aligned}
\tag{15}
$$

Figure 1 illustrates the pseudo code implemented to evaluate Equation 15. Figure 1 shows that, while the two nested loops [1] and [2] associated with process models remain, the quasi-MC method removes the two nested loops related to model parameters. Only one loop (i.e., loop [3] in Figure 1) is required to generate N samples for

each of the following three parameters: $\theta_{\sim K_q}$ of $M_{\sim K_q}$, θ_{K_p} of M_{K_p}, and $\theta_{K_p}{}'$ of M_{K_p}. To estimate index PS_{TK} related to a system process, model output $\Delta|\theta_{K_p}^{(j)}, M_{K_p}, \theta_{\sim K_q}^{(j)}, M_{\sim K_q}$ is evaluated upon running the system model (denoted as $M_{Kp} \cup M_{\sim Kq}$) for N times on the basis of the N samples of θ_{K_p} and $\theta_{\sim K_q}$. Model output $\Delta|\theta_{K_p}^{(j)}{}', M_{K_p}, \theta_{\sim K_q}^{(j)}, M_{\sim K_q}$ is evaluated by running the same system model ($M_{Kp} \cup M_{\sim Kq}$) for N times on the basis of the N samples of $\theta_{K_p}{}'$ and $\theta_{\sim K_q}$. In Figure 1, subscripts r and p of $\Delta|\theta_{K_r}^{(j)}, M_{K_r}, \theta_{\sim K_q}^{(j)}, M_{\sim K_q}$ and $\Delta|\theta_{K_p}^{(j)}, M_{K_p}, \theta_{\sim K_q}^{(j)}, M_{\sim K_q}$ denote different realizations of model M_K (of process K) and its model parameters θ_K. For computing $\left(\Delta|\theta_{K_p}^{(j)}, M_{K_p}, \theta_{\sim K_q}^{(j)}, M_{\sim K_q}\right) \times \left(\Delta|\theta_{K_r}^{(j)}, M_{K_r}, \theta_{\sim K_q}^{(j)}, M_{\sim K_q}\right)$ after Loop [3], one only needs to take two different realizations of the model output obtained in Loop [3], while there is no need to re-compute both $\Delta|\theta_{K_r}^{(j)}, M_{K_r}, \theta_{\sim K_q}^{(j)}, M_{\sim K_q}$ and $\Delta|\theta_{K_p}^{(j)}, M_{K_p}, \theta_{\sim K_q}^{(j)}, M_{\sim K_q}$. Therefore, the total number of model executions is $(m_{\sim k} \times m_k) \times 2N$.

2.3. Concurrent Estimation of PS_K and PS_{TK}

The approach we consider to concurrently estimating PS_K and PS_{TK} is patterned along the method developed by Saltelli et al. (2010) for the concurrent estimation of the first-order parameter sensitivity index, S_i, and the total-effect parameter sensitivity, S_{Ti}. It essentially relies on the use of three sample matrices, termed **A**, **B**, and $\mathbf{C}_i$. In Saltelli et al. (2010), entries of matrices **A** and **B** correspond to independently generated parameter samples. Each of these matrices is characterized by N rows and v columns, with N and v corresponding to the number of parameter realizations and number of model parameters, respectively. For the i-th parameter, matrix $\mathbf{C}_i$ is a copy of matrix **A** within which the i-th column is replaced with the corresponding column of matrix **B**. Using the parameter samples forming the entries of **A**, **B**, and $\mathbf{C}_i$, a system model is executed 3N times, the corresponding model outputs being denoted as $\mathbf{\Delta_A}$, $\mathbf{\Delta_B}$, and $\mathbf{\Delta_{C_i}}$, respectively (each of these is a vector with N elements). Sensitivity indices S_i and S_{Ti} of the i-th parameter are then evaluated via (Saltelli et al., 2010):

$$S_i = \frac{V_{\boldsymbol{\theta}_i}\left(E_{\boldsymbol{\theta}_{\sim i}}(\Delta|\theta_i)\right)}{V(\Delta)} \approx \frac{\frac{1}{N}\sum_{j=1}^{N} \Delta_{\mathbf{B}}{}^{(j)} \Delta_{\mathbf{C}_i}{}^{(j)} - \left(\frac{1}{N}\sum_{j=1}^{N} \Delta_{\mathbf{A}}{}^{(j)}\right)^2}{V(\Delta)}. \tag{16}$$

$$S_{Ti} = 1 - \frac{V_{\boldsymbol{\theta}_{\sim i}}\left(E_{\boldsymbol{\theta}_i}(\Delta|\theta_{\sim i})\right)}{V(\Delta)} \approx 1 - \frac{\frac{1}{N}\sum_{j=1}^{N} \Delta_{\mathbf{A}}{}^{(j)} \Delta_{\mathbf{C}_i}{}^{(j)} - \left(\frac{1}{N}\sum_{j=1}^{N} \Delta_{\mathbf{A}}{}^{(j)}\right)^2}{V(\Delta)}. \tag{17}$$

Here, $\Delta_{\mathbf{A}}{}^{(j)}$, $\Delta_{\mathbf{B}}{}^{(j)}$, and $\Delta_{\mathbf{C}_i}{}^{(j)}$ denote the j-th entries in $\mathbf{\Delta_A}$, $\mathbf{\Delta_B}$, and $\mathbf{\Delta_{C_i}}$, respectively. We note that $\mathbf{\Delta_A}$ and $\mathbf{\Delta_B}$ remain the same when one tackles the estimation of S_i and S_{Ti} related to another parameter. Otherwise, a new vector $\mathbf{\Delta_{C_i}}$ is needed. This is obtained by (a) generating a new matrix $\mathbf{C}_i$ and (b) running the system model for additional N times. Hence, concurrent estimation of S_i and S_{Ti} for all model parameters requires a total of $N \times (v + 2)$ model executions, where $N \times v$ corresponds to $\mathbf{C}_i$ ($i = 1, 2, \ldots, v$) and the remaining $N + N$ executions are for **A** and **B**, respectively.

Here, we also rely on matrix notations of **A**, **B**, and $\mathbf{C}_k$ (note that $\mathbf{C}_k$ is used to represent the kth process, instead of $\mathbf{C}_i$, to distinguish it from the ith parameter) for the concurrent estimation of process sensitivity indices PS_K and PS_{TK}. Otherwise, we would need to re-design and re-interpret these matrices in the context of model and parameter uncertainty. Matrices **A** and **B** are still characterized by N rows (for N parameter realizations) and v columns (for v parameters) for each system model. Note that the number of model parameters (v) can differ across system models. Matrix $\mathbf{C}_k$ ($k = 1, 2, \ldots, N_p$) is constructed for the kth process for each system model. Matrix $\mathbf{C}_k$ is still a copy of **A**, where all columns related to the parameters of the k-th process are replaced with the corresponding columns of matrix **B**. An example of constructing the three matrices is provided in Section 3 for a groundwater-related example. The three model output vectors generated for system model $M_{Kp} \cup M_{\sim Kq}$ using these three matrices are denoted as $\mathbf{\Delta_A}$, $\mathbf{\Delta_B}$, and $\mathbf{\Delta_{C_k}}$, respectively.

Equation 15 employed to estimate the total-effect process sensitivity index, PS_{TK}, can then be recast as:

$$V_{\mathbf{M}_{\sim K}}\left(E_{\mathbf{M}_K}\left(\Delta|M_{\sim K}\right)\right) \approx \sum_{q=1}^{m_{\sim K}}\sum_{p=1}^{m_K}\frac{1}{N}\sum_{j=1}^{N}\left(\Delta_{\mathbf{A}}^{(j)}\times\Delta_{\mathbf{C}_k}^{(j)}\right)P(M_{K_p})^2P\left(M_{\sim K_q}\right) + \sum_{q=1}^{m_{\sim K}}\sum_{p=1}^{m_K}\sum_{\substack{r=1\\ r\neq p}}^{m_K}\frac{1}{N}\sum_{j=1}^{N}\left(\Delta_{\mathbf{A}}^{(j)}\times\Delta_{\mathbf{A}_r}^{(j)}\right)P(M_{K_r})P(M_{K_p})P\left(M_{\sim K_q}\right), - \left(\sum_{q=1}^{m_{\sim K}}\sum_{p=1}^{m_K}\frac{1}{N}\sum_{j=1}^{N}\Delta_{\mathbf{A}}^{(j)}P\left(M_{\sim K_q}\right)P(M_{K_p})\right)^2 \tag{18}$$

Here, $\mathbf{\Delta}_{\mathbf{A}_r}$ denotes the vector of model output generated by matrix $\mathbf{A}$ of a different system model $M_{Kr} \cup M_{\sim Kq}$; and $\Delta_{\mathbf{A}}^{(j)}$, $\Delta_{\mathbf{A}_r}^{(j)}$, and $\Delta_{\mathbf{C}_k}^{(j)}$ denote the j-th entries in $\mathbf{\Delta}_{\mathbf{A}}$, $\mathbf{\Delta}_{\mathbf{A}_r}$, and $\mathbf{\Delta}_{\mathbf{C}_k}$, respectively. Equation 18 is a simplified expression of Equation 15 which is obtained by replacing $\Delta|\theta_{K_p}^{(j)}, M_{K_p}, \theta_{\sim K_q}^{(j)}, M_{\sim K_q}$, $\Delta|\theta_{K_r}^{(j)}, M_{K_r}, \theta_{\sim K_q}^{(j)}, M_{\sim K_q}$, and $\Delta|\theta_{K_p}^{(j)\prime}, M_{K_p}, \theta_{\sim K_q}^{(j)}, M_{\sim K_q}$ with $\Delta_{\mathbf{A}}^{(j)}$, $\Delta_{\mathbf{A}_r}^{(j)}$, and $\Delta_{\mathbf{C}_k}^{(j)}$, respectively. Similarly, the term $V_{\mathbf{M}_K}\left(E_{\mathbf{M}_{\sim K}}(\Delta|M_K)\right)$ appearing in Equation 1 and related to the estimation of the first-order process sensitivity index, PS_K, can be rewritten as:

$$V_{\mathbf{M}_K}\left(E_{\mathbf{M}_{\sim K}}(\Delta|M_K)\right) \approx \sum_{p=1}^{m_K}\sum_{q=1}^{m_{\sim K}}\frac{1}{N}\sum_{j=1}^{N}\left(\Delta_{\mathbf{B}}^{(j)}\times\Delta_{\mathbf{C}_k}^{(j)}\right)P\left(M_{\sim K_q}\right)^2P(M_{K_p}) + \sum_{p=1}^{m_K}\sum_{q=1}^{m_{\sim K}}\sum_{\substack{s=1\\ s\neq q}}^{m_{\sim K}}\frac{1}{N}\sum_{j=1}^{N}\left(\Delta_{\mathbf{B}}^{(j)}\times\Delta_{\mathbf{B}_s}^{(j)}\right)P\left(M_{\sim K_s}\right)P\left(M_{\sim K_q}\right)P(M_{K_p}), - \left(\sum_{p=1}^{m_K}\sum_{q=1}^{m_{\sim K}}\frac{1}{N}\sum_{j=1}^{N}\Delta_{\mathbf{B}}^{(j)}P\left(M_{\sim K_q}\right)P(M_{K_p})\right)^2 \tag{19}$$

Here, $\mathbf{\Delta}_{\mathbf{B}_s}$ denotes the vector of model output generated by matrix $\mathbf{B}$ of a different system model system model $M_{Kp} \cup M_{\sim Ks}$; $\Delta_{\mathbf{B}}^{(j)}$, $\Delta_{\mathbf{B}_s}^{(j)}$, and $\Delta_{\mathbf{C}_k}^{(j)}$ denote the j-th entries in $\mathbf{\Delta}_{\mathbf{B}}$, $\mathbf{\Delta}_{\mathbf{B}_s}$, and $\mathbf{\Delta}_{\mathbf{C}_k}$, respectively.

Equations 18 and 19 demonstrate that indices PS_K and PS_{TK} related to system process K can be concurrently estimated upon relying on sampling matrices $\mathbf{A}$, $\mathbf{B}$, and $\mathbf{C}_k$ at the computational cost of $(m_K \times m_{\sim K}) \times 3N$ (where $(m_K \times m_{\sim K})$ is the number of system models, and N is the number of parameter realizations for each system model). Estimating these two indices for another system process does not require constructing new matrices $\mathbf{A}$ and $\mathbf{B}$. It otherwise requires generating a new matrix $\mathbf{C}_k$. Therefore, concurrently estimating PS_K and PS_{TK} for all system processes requires a total of $(m_K \times m_{\sim K}) \times N \times (N_p + 2)$ model executions, where N_p is the number of system processes of interest (i.e., corresponding to the number of matrices $\boldsymbol{C}_k$), and the additional number 2 is for matrices $\mathbf{A}$ and $\mathbf{B}$.

The last term, $\left(\sum_{q=1}^{m_{\sim K}}\sum_{p=1}^{m_K}\frac{1}{N}\sum_{j=1}^{N}\Delta_{\mathbf{A}}^{(j)}P\left(M_{\sim K_q}\right)P(M_{K_p})\right)^2$, appearing at the right-hand side of Equation 18 and the last term, $\left(\sum_{p=1}^{m_K}\sum_{q=1}^{m_{\sim K}}\frac{1}{N}\sum_{j=1}^{N}\Delta_{\mathbf{B}}^{(j)}P\left(M_{\sim K_q}\right)P(M_{K_p})\right)^2$, at the right-hand of Equation 19 serve for evaluating $(E(\Delta))^2$. While these two terms theoretically coincide, their numerical MC counterparts might differ slightly because the former term uses $\mathbf{\Delta}_{\mathbf{A}}$ and the latter term uses $\mathbf{\Delta}_{\mathbf{B}}$. The variance term $V(\Delta)$ in Equations 1 and 2 is evaluated as:

$$V(\Delta) = E\left(\Delta^2\right) - (E(\Delta))^2 \approx \left(\sum_{p=1}^{m_K}\sum_{q=1}^{m_{\sim K}}\frac{1}{N}\sum_{j=1}^{N}\Delta_{\mathbf{A}}^{(j)^2}P\left(M_{\sim K_q}\right)P(M_{K_p})\right) - \left(\sum_{p=1}^{m_K}\sum_{q=1}^{m_{\sim K}}\frac{1}{N}\sum_{j=1}^{N}\Delta_{\mathbf{A}}^{(j)}P\left(M_{\sim K_q}\right)P(M_{K_p})\right)^2. \tag{20}$$

Such variance can also be evaluated upon relying on matrix $\mathbf{B}$. Similar to what stated above, while results based on the use of matrices $\mathbf{A}$ or $\mathbf{B}$ theoretically coincide, their numerical MC counterparts might differ slightly. Figure 2

illustrates the pseudo code implemented for the concurrent estimate of PS_K and PS_{TK} of process K on the basis of Equations 18 and 19. The first two loops are related to evaluating $\mathbf{\Delta_A}$, $\mathbf{\Delta_B}$, and $\mathbf{\Delta_{C_k}}$ needed for estimating PS_K and PS_{TK}. Loops [3] and [4] are related to estimating PS_{TK} based on Equation 18, loops [5] and [6] being related to evaluating PS_K through Equation 19. In Figure 2, $\mathbf{\Delta_{A_r}}$ used in Equation 18 and $\mathbf{\Delta_{B_s}}$ in Equation 19 are vectors of model output generated by matrices $\mathbf{A}$ and $\mathbf{B}$ of system models $M_{Kr} \cup M_{\sim Kq}$ and $M_{Kp} \cup M_{\sim Ks}$. For computing $\left(\Delta_{\mathbf{A}}^{(j)}\right) \times \left(\Delta_{\mathbf{A}_r}^{(j)}\right)$ in Loop [4] and $\left(\Delta_{\mathbf{B}}^{(j)}\right) \times \left(\Delta_{\mathbf{B}_s}^{(j)}\right)$ in Loop [6], one only needs to take two different indices of the model output obtained in Loop [2], and there is no need to re-compute both $\Delta_{\mathbf{A}_r}^{(j)}$ and $\Delta_{\mathbf{B}_s}^{(j)}$. Therefore, the total number of model executions is $(m_{\sim k} \times m_k) \times 3N$.

3. Assessment of the Quasi-MC Method for Concurrent Estimation of PS_K and PS_{TK}

3.1. One-Dimensional Groundwater Flow Scenario

To provide a transparent assessment of our methodological and theoretical approach, we rely on a synthetic scenario of the one-dimensional (1-D) groundwater modeling that has been used in previous studies focusing on process model uncertainty analysis (Dai & Ye, 2015; Dai et al., 2024; Yang et al., 2022). Figure 3 illustrates the 1-D domain of the exemplary groundwater flow setting. We mimic an unconfined aquifer characterized by a length of $L = 10{,}000$ m within which steady state flow takes place. Constant-head boundary conditions are imposed on the left and right sides of the aquifer. A constant head of 300 m is set at the left boundary, and the right boundary corresponding to a river with a constant river stage, that is, determined using a hypothetical rating curve based on a snowmelt process. In addition to the snowmelt process, the groundwater flow scenario also embeds a geological process for the aquifer hydraulic conductivity and a recharge process to quantify aquifer recharge from precipitation.

Each process is represented by two process models, all of which are listed in Table 1. The two recharge models (denoted as R_1 and R_2) estimate recharge from precipitation by using two empirical equations. For the two geological models, the hydraulic conductivity of the aquifer can be either homogenous (denoted as G_1) for the entire aquifer or zonal-heterogeneous (denoted as G_2) with two zones deterministically demarcated at location $x_0 = 7{,}000$ m. The two snowmelt models (denoted as S_1 and S_2) provide estimates of the amount of snowmelt through two empirical formulations. Equal weights are assumed for alternative process models (e.g., $P(R_1) = P(R_2) = 0.5$), with process model weights being listed in Table 1. Impacts of process model weights on estimation of PS_K and PS_{TK} are discussed in Section 4. In addition to the process models, Table 1 also lists the uncertain parameters and their associated PDFs considered in our study. The quantity of interest Δ is the groundwater discharge per unit width at $x_0 = 7{,}000$ m. Since each process has two alternative process models (Table 1), there are a total of eight ($8 = 2 \times 2 \times 2$) system models. These are hereafter denoted as $R_1G_1S_1$, $R_1G_1S_2$, $R_1G_2S_1$, $R_1G_2S_2$, $R_2G_1S_1$, $R_2G_1S_2$, $R_2G_2S_1$, and $R_2G_2S_2$. Each system model has three to five uncertain parameters (e.g., three in $R_1G_1S_1$ and five in $R_2G_2S_2$).

3.2. Sampling Matrices for Concurrent Estimation of PS_K and PS_{TK}

Here, we illustrate the procedure employed to generate matrices $\mathbf{A}$, $\mathbf{B}$, and $\mathbf{C}_k$ within the context of the exemplary setting described in Section 3.1. For each system model, matrix $\mathbf{A}$ can be generated using any sequence of quasi-random numbers, Sobol' sequences being used in this study based on the PDFs $p(\theta_{K_p}|M_{K_p})$ and $p\left(\theta_{\sim K_q}\middle|M_{\sim K_q}\right)$ listed in Table 1. Matrix $\mathbf{B}$ is independently generated according to the same procedure. Parameters are arranged in the same order in matrices $\mathbf{A}$ and $\mathbf{B}$, which is a requirement for generating matrix $\mathbf{C}_k$. Considering system model $R_1G_2S_2$ as an example, its random parameters include a for recharge model R_1, HK_1 and HK_2 for geological model G_2, and f_2 and r for snowmelt model S_2. Matrices $\mathbf{A}$ and $\mathbf{B}$ associated with the model are:

$$\mathbf{A} = \begin{bmatrix} a^{(1)} & HK_1{}^{(1)} & HK_2{}^{(1)} & f_2{}^{(1)} & r^{(1)} \\ a^{(2)} & HK_1{}^{(2)} & HK_2{}^{(1)} & f_2{}^{(1)} & r^{(2)} \\ \cdots & \cdots & \cdots & \cdots & \cdots \\ a^{(N)} & HK_1{}^{(N)} & HK_2{}^{(N)} & f_2{}^{(N)} & r^{(N)} \end{bmatrix}, \tag{21}$$

Loop [1] over $(m_K \times m_{\sim K})$ system models $M_{Kp} \bigcup M_{\sim Kq}$ in $\mathbf{M}_K \bigcup \mathbf{M}_{\sim K}$

Loop [2] over N parameter realizations in sample matrices **A**, **B**, and $\mathbf{C}_k$

Compute $\Delta_{\mathbf{A}}^{(j)}$, $\Delta_{\mathbf{B}}^{(j)}$, and $\Delta_{\mathbf{C}_k}^{(j)}$

End Loop [2]

End Loop [1]

Loop [3] over $m_{\sim K}$ process models $M_{\sim K}$ of process $\sim K$ in $\mathbf{M}_{\sim K}$

Loop [4] over m_K process models M_K of process K in $\mathbf{M}_K$

Compute $\frac{1}{N}\sum_{j=1}^{N}\left(\Delta_{\mathbf{A}}^{(j)} \times \Delta_{\mathbf{C}_k}^{(j)}\right)$, $\frac{1}{N}\sum_{j=1}^{N}\left(\Delta_{\mathbf{A}}^{(j)} \times \Delta_{\mathbf{A}_r}^{(j)}\right)$, and $\frac{1}{N}\sum_{j=1}^{N}\Delta_{\mathbf{A}}^{(j)}$

End Loop [4]

Compute $\sum_{p=1}^{m_K}\frac{1}{N}\sum_{j=1}^{N}\left(\Delta_{\mathbf{A}}^{(j)} \times \Delta_{\mathbf{C}_k}^{(j)}\right)P(M_{K_p})^2$,

$\sum_{p=1}^{m_K}\sum_{\substack{r=1 \\ r\neq p}}^{m_K}\frac{1}{N}\sum_{j=1}^{N}\left(\Delta_{\mathbf{A}}^{(j)} \times \Delta_{\mathbf{A}_r}^{(j)}\right)P(M_{K_r})P(M_{K_p})$, and $\sum_{p=1}^{m_K}\frac{1}{N}\sum_{j=1}^{N}\Delta_{\mathbf{A}}^{(j)}P\left(M_{K_p}\right)$

End Loop [3]

Compute $\sum_{q=1}^{m_{\sim K}}\sum_{p=1}^{m_K}\frac{1}{N}\sum_{j=1}^{N}\left(\Delta_{\mathbf{A}}^{(j)} \times \Delta_{\mathbf{C}_k}^{(j)}\right)P(M_{K_p})^2 P(M_{\sim K_q})$, $\sum_{q=1}^{m_{\sim K}}\sum_{p=1}^{m_K}\sum_{\substack{r=1 \\ r\neq p}}^{m_K}\frac{1}{N}\sum_{j=1}^{N}\left(\Delta_{\mathbf{A}}^{(j)} \times \Delta_{\mathbf{A}_r}^{(j)}\right)P(M_{K_r})P(M_{K_p})P(M_{\sim K_q})$,

and $\left(\sum_{q=1}^{m_{\sim K}}\sum_{p=1}^{m_K}\frac{1}{N}\sum_{j=1}^{N}\Delta_{\mathbf{A}}^{(j)}P\left(M_{\sim K_q}\right)P\left(M_{K_p}\right)\right)^2$

Loop [5] over m_K process models M_K of process K in $\mathbf{M}_K$

Loop [6] over $m_{\sim K}$ process models $M_{\sim K}$ of process $\sim K$ in $\mathbf{M}_{\sim K}$

Compute $\frac{1}{N}\sum_{j=1}^{N}\left(\Delta_{\mathbf{B}}^{(j)} \times \Delta_{\mathbf{C}_k}^{(j)}\right)$, $\frac{1}{N}\sum_{j=1}^{N}\left(\Delta_{\mathbf{B}}^{(j)} \times \Delta_{\mathbf{B}_s}^{(j)}\right)$, and $\frac{1}{N}\sum_{j=1}^{N}\Delta_{\mathbf{B}}^{(j)}$

End Loop [6]

Compute $\sum_{q=1}^{m_{\sim K}}\frac{1}{N}\sum_{j=1}^{N}\left(\Delta_{\mathbf{B}}^{(j)} \times \Delta_{\mathbf{C}_k}^{(j)}\right)P\left(M_{\sim K_q}\right)^2$, $\sum_{q=1}^{m_{\sim K}}\sum_{\substack{s=1 \\ s\neq q}}^{m_{\sim K}}\frac{1}{N}\sum_{j=1}^{N}\left(\Delta_{\mathbf{B}}^{(j)} \times \Delta_{\mathbf{B}_s}^{(j)}\right)P\left(M_{\sim K_s}\right)P\left(M_{\sim K_q}\right)$,

and $\sum_{q=1}^{m_{\sim K}}\frac{1}{N}\sum_{j=1}^{N}\Delta_{\mathbf{B}}^{(j)}P\left(M_{\sim K_q}\right)$

End Loop [5]

Compute $\sum_{p=1}^{m_K}\sum_{q=1}^{m_{\sim K}}\frac{1}{N}\sum_{j=1}^{N}\left(\Delta_{\mathbf{B}}^{(j)} \times \Delta_{\mathbf{C}_k}^{(j)}\right)P\left(M_{\sim K_q}\right)^2 P\left(M_{K_p}\right)$, $\sum_{p=1}^{m_K}\sum_{q=1}^{m_{\sim K}}\sum_{\substack{s=1 \\ s\neq q}}^{m_{\sim K}}\frac{1}{N}\sum_{j=1}^{N}\left(\Delta_{\mathbf{B}}^{(j)} \times \Delta_{\mathbf{B}_s}^{(j)}\right)P\left(M_{\sim K_s}\right)P\left(M_{\sim K_q}\right)P\left(M_{K_p}\right)$,

and $\left(\sum_{p=1}^{m_K}\sum_{q=1}^{m_{\sim K}}\frac{1}{N}\sum_{j=1}^{N}\Delta_{\mathbf{B}}^{(j)}P\left(M_{\sim K_q}\right)P\left(M_{K_p}\right)\right)^2$

Figure 2. Pseudo code developed for the concurrent estimation of PS_K and PS_{TK} based on Equations 18 and 19.

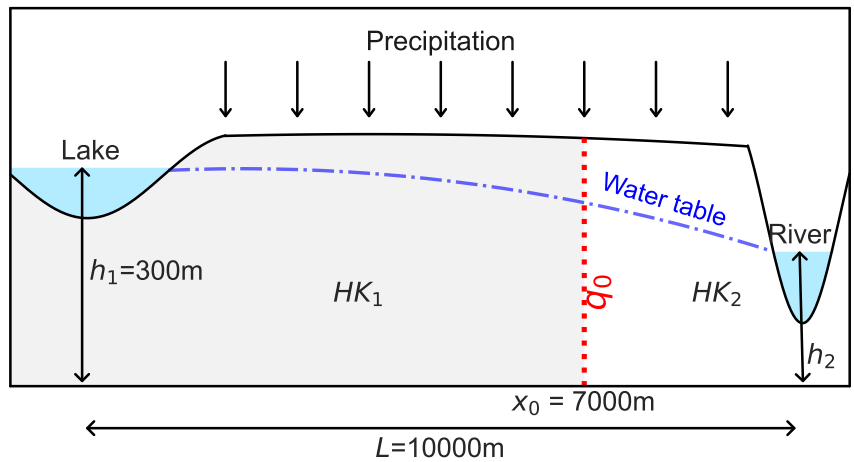

Figure 3. Sketch of the modeling domain considered, including main geometrical features and boundary conditions. The demarcation of the two regions with differing hydraulic conductivity values considered in one of the representations of the geological setting is highlighted (vertical red dashed line).

$$\mathbf{B} = \begin{bmatrix} a'^{(1)} & HK_1'^{(1)} & HK_2'^{(1)} & f_2'^{(1)} & r'^{(1)} \\ a'^{(2)} & HK_1'^{(2)} & HK_2'^{(1)} & f_2'^{(1)} & r'^{(2)} \\ \cdots & \cdots & \cdots & \cdots & \cdots \\ a'^{(N)} & HK_1'^{(N)} & HK_2'^{(N)} & f_2'^{(N)} & r'^{(N)} \end{bmatrix}. \tag{22}$$

For each system model, matrix $\mathbf{C}_k$ is generated by replacing columns for the parameters of the k-th process in matrix **A** by the corresponding columns of matrix **B**. Taking $R_1G_2S_2$ as an example, matrix $\mathbf{C}_3$ associated with the snowmelt process (i.e., the third process) is:

Table 1
Alternative Process Models, Corresponding Model Parameters, and Parameter PDFs of the Recharge, Geology, and Snowmelt Processes of the 1-D Groundwater Flow System Depicted in Figure 3

Processes name	Process model representation	Model weight	Uncertain parameter	
			Name	PDFs[a]
Recharge	$R_1 : w = a(PCP - 14)^{0.5} \times 0.0254/365$	0.5	a	N (2.0, 0.4^2)
	$R_2 : w = b(PCP - 15.7) \times 0.0254/365$	0.5	b	U (0.2, 0.5)
Geology	$G_1 : HK$ for any x	0.5	HK	LN (2.9, 0.5^2)
	$G_2 : HK = \begin{cases} HK_1 & \text{for } x < 7000 \\ HK_2 & \text{for } x \geq 7000 \end{cases}$	0.5	HK_1	LN (2.6, 0.3^2)
			HK_2	LN (3.2, 0.3^2)
Snowmelt	$S_1 : S = f_1(T_a - T_m)$	0.5	f_1	N (3.5, 0.75^2)
	$S_2 : S = f_2(T_a - T_m) + rR_n$	0.5	f_2	N (2.5, 0.3^2)
			r	N (0.3, 0.05^2)

Sensitivity indices	Recharge	Geology	Snowmelt
PS_K	0.1456	0.0699	0.6411
PS_{TK}	0.1490	0.2133	0.7811

Note. The sensitivity indices of the three processes listed here are reference values that are estimated using a sufficiently large number (8 billion) of model executions. [a]N denotes a normal distribution, U a uniform distribution, and LN a (natural) lognormal distribution. Parameter PCP is the annual precipitation, T_a is the average temperature, T_m is the temperature threshold when snow melt takes place, and R_n is the surface radiation budget. The values of these parameters are deterministic, and they are PCP = 60 inch/year, T_a = 7°C, T_m = 0°C, and R_n = 80 W/m^2.

$$\mathbf{C}_3 = \begin{bmatrix} a^{(1)} & HK_1{}^{(1)} & HK_2{}^{(1)} & f_2{}'^{(1)} & r'^{(1)} \\ a^{(2)} & HK_1{}^{(2)} & HK_2{}^{(1)} & f_2{}'^{(1)} & r'^{(2)} \\ \cdots & \cdots & \cdots & \cdots & \cdots \\ a^{(N)} & HK_1{}^{(N)} & HK_2{}^{(N)} & f_2{}'^{(N)} & r'^{(N)} \end{bmatrix}. \quad (23)$$

When generating matrices **A** and **B** for different system models (i.e., in loops [1] and [2] of Figure 2), it is noted that, if the two system models are characterized by different numbers of random parameters, then the size of matrix **A** varies across these diverse system models. The matrix dimension is $N \times v$, where N is the number of parameter samples and v is the number of random parameters, corresponding to the number of columns of **A**. We further note that v can vary between different system models, each being associated with a given number of random parameters. If two system models are characterized by some common parameters, parameter samples need to be the same for the two system models. This requirement is set to ensure that model output Δ is conditioned on the same parameter samples, as indicated by Equation 15. For instance, system models $R_1G_1S_1$ and $R_1G_1S_2$ share parameters a for process model R_1 and HK for process model G_1. Hence, the columns of matrix **A** for parameters a and HK are the same for these system models. Generally speaking, the number of parameter samples in matrices **A** and **B** cannot be assessed a priori. One needs to carefully examine convergence and accuracy of the quasi-MC simulations for estimating the process sensitivity indices. This is especially critical in settings with a large number of model parameters, complex probability distributions of model parameters, and high model nonlinearity and complex parameter interactions.

3.3. Convergence and Accuracy

To evaluate convergence of the quasi-MC method developed here, reference values for PS_K and PS_{TK} related to the three processes considered are obtained upon relying on the brute force MC method implemented through a large number of parameter samples. The ensuing reference values are listed in Table 1, as a result of a total number of model executions equal to $8 \times 10^9 = 2 \times 1{,}000 \times 2 \times 1{,}000 \times 2 \times 1{,}000$, corresponding to 2 recharge process models × 1,000 parameter samples × 2 geology process models × 1,000 parameter samples × 2 snowmelt process models × 1,000 parameter samples. This is equivalent to $(2 \times 1{,}000) \times (2^2 \times 10{,}00^2)$ model executions for estimating PS_K and $(2^2 \times 10{,}00^2) \times (2 \times 1{,}000)$ model executions for estimating PS_{TK} using the brute force MC method. While reliance on 8 billion model executions ensures accurate estimates of PS_K and PS_{TK}, doing so is not strictly necessary in practice, because the estimated PS_K and PS_{TK} values are seen to converge after several million model executions (Figure 4).

Using the reference values (Table 1), absolute relative errors (%) associated with the implementation of our quasi-MC method were evaluated. Figure 4 depicts these as a function of the number of model simulations for the two process sensitivity indices of the three processes. These results reveal that the quasi-MC method converges substantially faster than the brute force MC method for PS_K and PS_{TK} of all three processes. For example, Figures 4a and 4d show that, when considering the evaluation of PS_K and PS_{TK} of the recharge process through brute force MC, the absolute relative errors become less than 1% after 4.4×10^8 model simulations. Otherwise, the corresponding number of simulations are 3.2×10^5 (Figure 4a) and 8.0×10^4 (Figure 4d) for evaluating PS_K and PS_{TK} of the recharge process, respectively, using our quasi-MC method. Hence, the estimation is about 1,000 times faster. Results of similar quality are found for the other two processes as well. On the other hand, our quasi-MC method yields more accurate results than its brute force MC counterparts when associated with the same number of model executions. Hence, we conclude that the quasi-MC method converges faster and is more accurate than the brute force MC method.

Evaluation of uncertainty in the estimation of the process sensitivity indices due to reliance on a limited number of parameter samples is performed through the quantification of bootstrap confidence intervals for the brute force MC and quasi-MC methods. We do so by following Nossent et al. (2011). While the bootstrapping procedure for the brute force MC method is straightforward, the procedure for the quasi-MC method comprises the steps described below:

1. Generate Sobol' sequences of N (e.g., 10, 1,010, 2,010, …, 500,010, starting with an initial value of 10 with the increment of 1,000) parameter samples for matrices **A**, **B**, and $\mathbf{C}_k$. The maximum number of 500,010 is

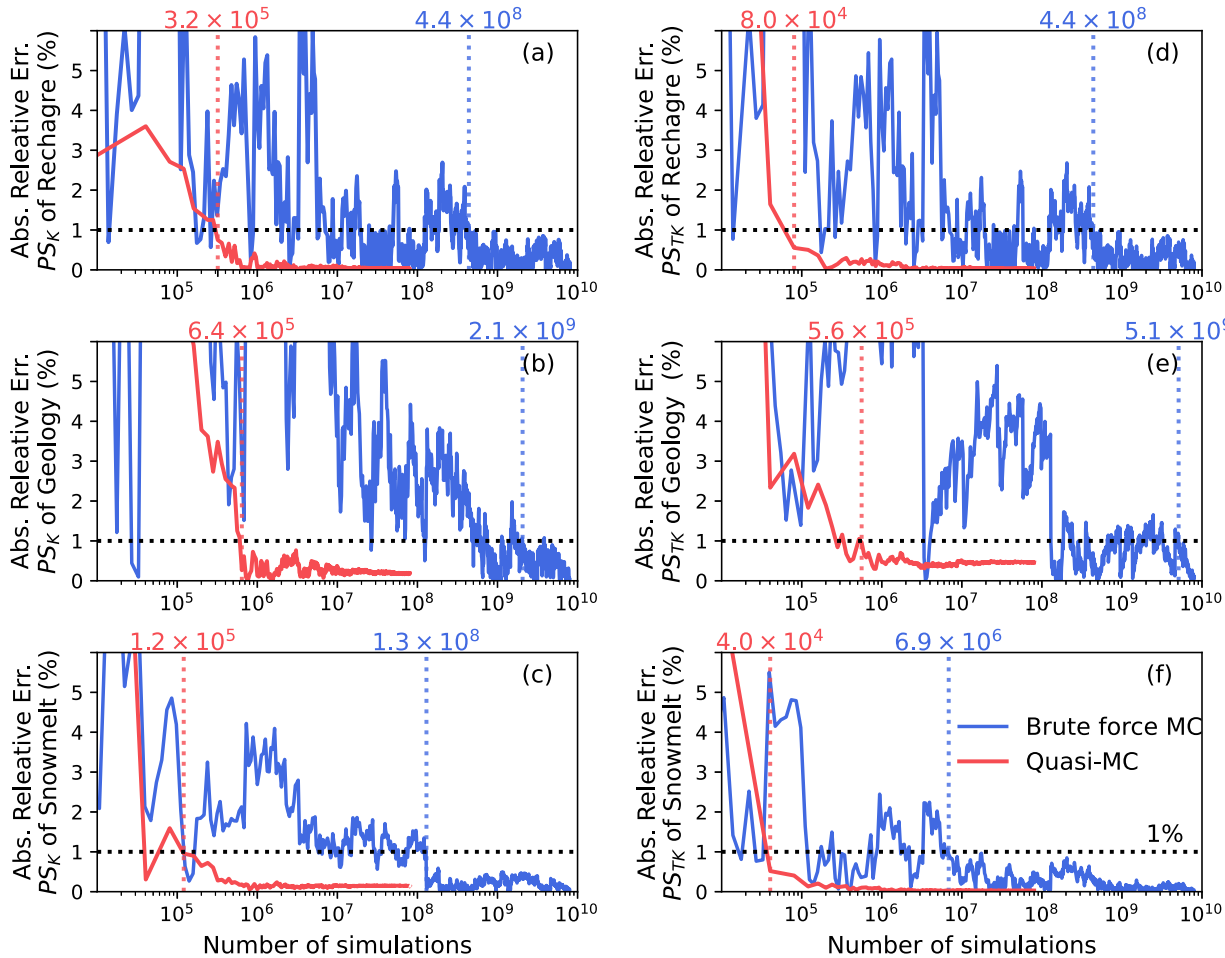

Figure 4. Convergence of absolute relative errors (%) for process sensitivity indices of (a–c) PS_K and (d–f) PS_{TK} for the recharge, geology, and snowmelt processes evaluated via brute force (solid blue curves) and quasi-MC (solid red curves) methods. The absolute relative errors (%) are plotted against the logarithm number of model simulations. Vertical dotted lines mark the number of simulations at which the errors fall below the 1% threshold for the brute force (blue) and quasi-MC (red) methods.

selected on the basis of Figure 4, as it is sufficiently large to ensure convergence of the quasi-MC method. The two process sensitivity indices, PS_K and PS_{TK}, of the three processes are evaluated for each collection of N parameter samples (a total of 40N model executions are required for each N), the corresponding results being depicted in Figure 5.

2. For each collection of N samples, generate N bootstrap replicas for matrices **A** and **B** and then generate matrix $\mathbf{C}_k$. Evaluate PS_K and PS_{TK} using these generated matrices. Note that the bootstrap replicas are no longer Sobol' sequence. However, the overall procedure (and algorithm) is still to be considered within the quasi-Monte Carlo framework because it yields a single expectation, as expressed through Equations 9 and 10.
3. For each set of N samples, repeat step (2) 100 times to yield 100 estimates of PS_K and PS_{TK} for the three processes. Then, evaluate the 95% confidence intervals of PS_K and PS_{TK} as $\mu \pm 1.96\,\sigma$, where μ and σ denote the mean and standard deviation of the 100 estimates, respectively.

The 95% confidence intervals stemming from the workflow illustrated above are depicted in Figure 5. The figure shows that the confidence intervals of the quasi-MC method are substantially narrower than their counterparts related to the brute force MC method for the two process sensitivity indices of all three processes. This finding suggests that the quasi-MC method results are more precise (and reliable) than their brute force MC counterparts.

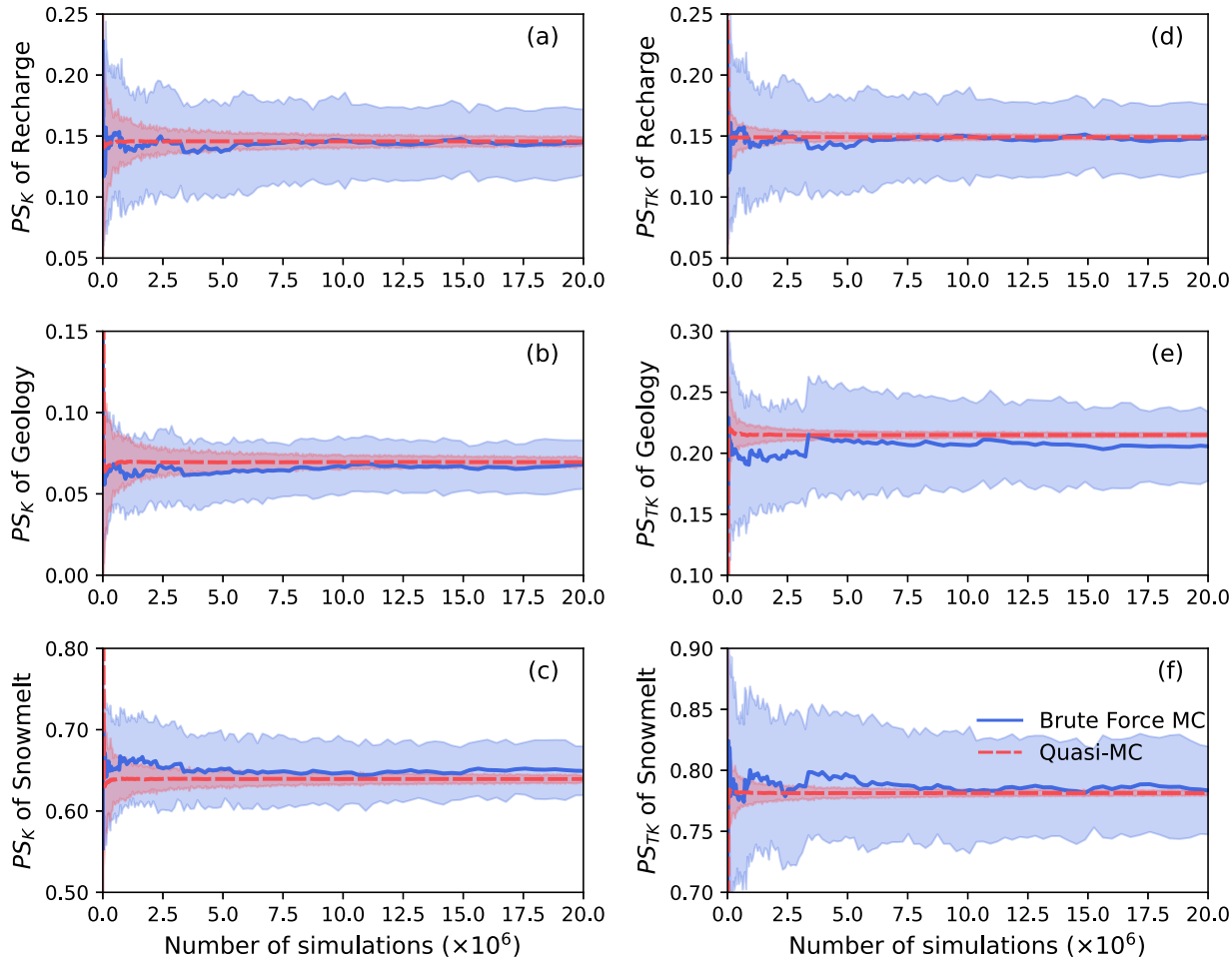

Figure 5. The 95% bootstrap confidence intervals associated with the evaluation of (a–c) PS_K and (d–f) PS_{TK} of the recharge, geology, and snowmelt processes. Solid blue and dashed red curves are related to the brute force MC and quasi-MC methods, respectively. Light blue and red areas correspond to 95% confidence intervals for the brute force MC and quasi-MC methods, respectively.

4. Discussion

4.1. Impacts of Process Model Weights on Estimation of PS_K and PS_{TK}

To investigate the impact of process model weights on estimation of PS_K and PS_{TK}, we consider a total of 2,000 sets of process model weights. In each set, a random value $P(R_1)$ associated with recharge model R_1 is drawn from the uniform distribution $U(0, 1)$. A corresponding value of $P(R_2)$ associated with recharge model R_2 is evaluated upon recalling that each process is represented by two process models with model weights that sum up to unity (i.e., $P(R_1) + P(R_2) = 1.0$). This procedure is repeated for the two geological models and the two snowmelt models. Values of PS_K and PS_{TK} are evaluated for each of the 2,000 sets of process model weights. Figure 6 illustrates the variation of PS_{TK} with $P(R_1)$, $P(G_1)$, and $P(S_1)$ for the recharge, geology, and snowmelt processes. The variation of PS_K with process model weights for the three processes is similar to that of PS_{TK}, and the results for PS_K are thus not shown. Figure 6 plots the marginal histograms of $P(R_1)$, $P(G_1)$, and $P(S_1)$ on the top of each subplot, and the histograms visually follow the uniform distribution $U(0, 1)$. This indicates that the 2,000 samples are adequate to represent the variation of the process model weights.

Trendlines included in Figure 6 show differing patterns of variability of PS_{TK} with process model weights. Taking the recharge process as an example, while PS_{TK} of recharge monotonically decreases with the increase of $P(R_1)$ and $P(G_1)$ (Figures 6a and 6b), PS_{TK} of recharge first decreases with $P(S_1)$ for $P(S_1) < 0.5$ and then increase for $P(S_1) > 0.5$ (Figure 6c). In addition, the variation pattern is different from the three processes. For example, the variation pattern of PS_{TK} for recharge is opposite to its counterpart associated with snowmelt (Figures 6c and 6i).

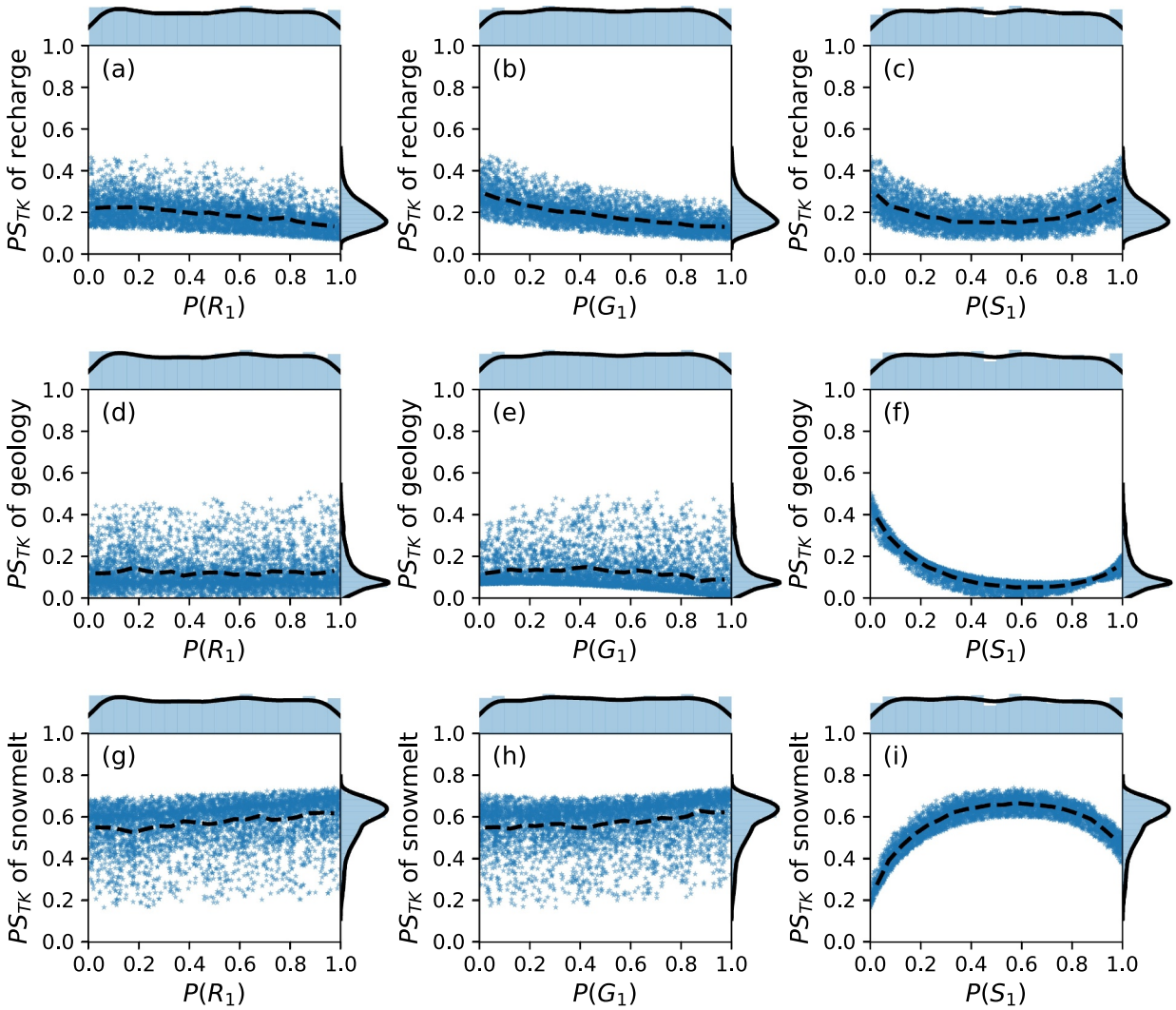

Figure 6. Variation of PS_{TK} with process model weights $P(R_1)$, $P(G_1)$, and $P(S_1)$ for (a–c) the recharge process, (d–f) the geology process, and (g–i) the snowmelt process. Dashed black curves correspond to trendlines of the PS_{TK} variation based on mean PS_{TK} values evaluated upon discretizing the horizontal axis through 20 bins. Solid black curves correspond to marginal histograms of $P(R_1)$, $P(G_1)$, $P(S_1)$, and PS_{TK}.

These results suggest that it is necessary to consider the impacts of process model weights on the estimation of PS_K and PS_{TK}.

The marginal histograms of PS_{TK} depicted in Figure 6 suggest that, even considering the above-mentioned variation of PS_{TK}, one can clearly conclude that the snowmelt process is the most influential process. This is related to the observation that values of PS_{TK} for the snowmelt process are in general larger than their counterparts associated with the other two processes. Yang et al. (2022) ascribed the high influence of the snowmelt process to high importance of the process (measured through PS_K shown in Figure 5) and the interaction between the snowmelt and the geology processes (see Figure 5 of Yang et al., 2022). The marginal histograms of PS_{TK} shown in Figure 6 indicate that the geology process is the least influential, values of PS_{TK} for such process being smaller overall than those related to the other two processes. This result is different from what one could infer from Figure 5, which shows that the value of PS_{TK} associated with the geological process is larger than that related to the recharge process. The difference should not be surprising, as the results embedded in Figure 5 are based on the equal weights (i.e., 0.5) for the two geological process models. The analysis of Figure 6 suggests that, given the impact of process model weights on the estimation of PS_K and PS_{TK}, one would need to determine the weights upon relying on all available information (e.g., expert elicitation).

4.2. Limitations and Future Studies

The process sensitivity indices and the quasi-MC method presented here are subject to some theoretical, computational, and practical limitations. Providing a rigorous theoretical assessment of these limitations is beyond the scope of this study, and is otherwise the subject of future studies. The theoretical limitation is that the process sensitivity indices cannot quantify conceptual errors (e.g., missing an important process) related to developing the system models. In this study we do not investigate how system model errors affect the identification of important and/or influential processes. Here, we assume that all important system processes are considered in the system models, which might require an extensive data collection campaign for system states (e.g., hydraulic heads and solute concentrations) and comparison against corresponding model simulations. While the occurrence of substantial discrepancies between data and corresponding model simulations may indicate system model errors, the issue of errors cannot be addressed upon relying on process sensitivity indices. These limitations reflect the epistemic nature of model uncertainty and subjective decisions inherently involved in model formulation and evaluation. These should be made explicit, traceable, and reproducible (Page et al., 2023).

The work here presented is subject to two computational limitations. One limitation is that the estimation of the process sensitivity indices does not explicitly address the complexity of the process models. For example, snowmelt model S_2 is characterized by two parameters and thus is more complex than snowmelt model S_1 that has only one parameter. Hence, one might consider assigning different weights depending on model complexity. We recall that, while process model weights can be determined in various ways (e.g., expert elicitation), they must be determined before estimating the process sensitivity indices. As an additional computational limitation, we note that our study does not provide a general guideline on the selection of the number of parameter samples required for convergence of the quasi-MC method presented here. This limitation is typical of a variety of studies relying on numerical Monte Carlo simulations, as such a number of parameter samples depends on multiple factors, including the number of model parameters, probability distributions of the parameters, and the degree of model nonlinearity and parameter interactions. One must carefully examine convergence and accuracy of the quasi-MC method case by case.

The practical limitation is that the process sensitivity indices and the quasi-MC method have not yet been applied to complex, multi-dimensional systems or large-scale scenarios where system dynamics could be described through models that are often high-dimensional, involving numerous interconnected processes that vary significantly across space and time, with intricate feedback mechanisms. Our study (as well as the works of Dai et al. (2017, 2024) and Yang et al. (2022)) is focused on the development of theoretical methodologies and computational algorithms. Hence, we rely on simple settings for our tests. We further note that, even as process sensitivity indices and the quasi-MC method have been used for various ecological and hydrological modeling scenarios (Dai et al., 2019, 2024; Ju et al., 2021; Liu et al., 2020; Walker et al., 2018, 2021), none of these applications involve complex and multi-dimensional systems. Developing system models for such scenarios can be significantly more complex than constructing the simplified groundwater models upon which we rely for the purpose of our analyses, to the point that it might constitute a research topic in its own right. Furthermore, running numerical simulations of these models can be equally demanding, particularly when existing codes (such as, e.g., MODFLOW and MT3D-MS) must be adapted to accommodate alternative process representations. Although this issue may be mitigated upon resting on other simulation tools (e.g., PFLOTRAN (Hammond et al., 2014) for reactive transport modeling), applying process sensitivity indices to complex real-world systems still requires some compromises, critical assumptions, and simplifications to ensure that the indices can be computed with available codes and computational resources. Nevertheless, our studies clarify that relying on quantitative analyses embedding process sensitivity indices offers a novel approach for addressing process model uncertainty by identifying key and influential processes, and that quasi-Monte Carlo algorithms provide a computationally efficient means of simultaneously estimating both indices.

5. Conclusions

Our study is keyed to two major technical contributions to enhance computational aspects related to the evaluation of process sensitivity analysis in hydrological and Earth system scenarios. One contribution entails the development of the quasi-MC method to estimate the total-effect process sensitivity index, PS_{TK}. The method is patterned after the work of Dai et al. (2022), who considered estimation of the first-order process sensitivity index, PS_K, in that the two methods use three sets of parameter samples to remove two nested parameter samplings

required by the brute force MC method. This enables one to reduce the number of model executions from N^2 (for the brute force MC method) to N (for the quasi-MC method). Another significant computational contribution, which is unique to our study, is that the quasi-MC method is employed to concurrently estimate PS_K and PS_{TK}. Such a concurrent estimation is in the spirit of the work of Saltelli et al. (2010) aimed at estimating first-order and total-effect parameter sensitivity indies, but we extend their work to encompass first-order and total-effect process sensitivity indices while considering process model uncertainty. We obtain the simplified expressions of the quasi-MC method by using three sampling matrices $\mathbf{A}$, $\mathbf{B}$, and $\mathbf{C}_k$ for the concurrent estimation of the two process indices. The number of model execution required for the concurrent estimation of the two indices for all system processes is $(m_K \times m_{\sim K}) \times N \times (N_p + 2)$, where $(m_K \times m_{\sim K})$ is the number of system models, N is the number of parameter samples for each system model, and N_p is the number of system processes of interest. Convergence, accuracy, and reliability with respect to sampling uncertainty of our quasi-MC method are evaluated upon relying on an exemplary one-dimensional scenario involving groundwater flow. Our results demonstrate that the quasi-MC method converges substantially faster and is substantially more reliable than its brute force MC counterpart. Hence, our study sets the basis for future applications of the quasi-MC method for concurrently estimating the two process sensitivity indices to a wide range of process sensitivity analyses associated with process-based modeling scenarios. It should be noted that PS_K and PS_{TK} values are substantially affected by the process model weights, and it is necessary to determine appropriate weights by using available information through various means such as expert elicitation.

Conflict of Interest

The authors declare no conflicts of interest relevant to this study.

Data Availability Statement

All computer codes and data used in this study are available online at Zenodo via https://zenodo.org/records/14005950.

Acknowledgments
This study was supported by National Natural Science Foundation of China (Grants 42302288 and 42402245). Part of the study was conducted by J. Yang when he was a visiting student at the Florida State University. A. Guadagnini acknowledges funding from the European Union Next-Generation EU (National Recovery and Resilience Plan - NRRP, Mission 4, Component 2, Investment 1.3—D.D. 1243 2/8/2022, PE0000005) in the context of the RETURN Extended Partnership. The authors are grateful to the three anonymous reviewers for their constructive comments, which have greatly improved the quality of this manuscript.

References

Antonetti, M., Buss, R., Scherrer, S., Margreth, M., & Zappa, M. (2016). Mapping dominant runoff processes: An evaluation of different approaches using similarity measures and synthetic runoff simulations. *Hydrology and Earth System Sciences*, *20*(7), 2929–2945. https://doi.org/10.5194/hess-20-2929-2016

Ceriotti, G., Guadagnini, L., Porta, G., & Guadagnini, A. (2018). Local and global sensitivity analysis of Cr (VI) geogenic leakage under uncertain environmental conditions. *Water Resources Research*, *54*(8), 5785–5802. https://doi.org/10.1029/2018wr022857

Clark, M. P., Nijssen, B., Lundquist, J. D., Kavetski, D., Rupp, D. E., Woods, R. A., et al. (2015). A unified approach for process-based hydrologic modeling: 2. Model implementation and case studies. *Water Resources Research*, *51*(4), 2515–2542. https://doi.org/10.1002/2015wr017200

Dai, H., Chen, X., Ye, M., Song, X., Hammond, G., Hu, B. X., & Zachara, J. M. (2019). Using Bayesian networks for sensitivity analysis of complex biogeochemical models. *Water Resources Research*, *55*(4), 3541–3555. https://doi.org/10.1029/2018WR023589

Dai, H., Ju, J., Gui, D., Zhu, Y., Ye, M., Liu, Y., et al. (2024). A two-step Bayesian network-based process sensitivity analysis for complex nitrogen reactive transport modeling. *Journal of Hydrology*, *632*, 130903. https://doi.org/10.1016/j.jhydrol.2024.130903

Dai, H., & Ye, M. (2015). Variance-based global sensitivity analysis for multiple scenarios and models with implementation using sparse grid collocation. *Journal of Hydrology*, *528*, 286–300. https://doi.org/10.1016/j.jhydrol.2015.06.034

Dai, H., Ye, M., Walker, A. P., & Chen, X. (2017). A new process sensitivity index to identify important system processes under process model and parametric uncertainty. *Water Resources Research*, *53*(4), 3476–3490. https://doi.org/10.1002/2016wr019715

Dai, H., Zhang, F., Ye, M., Guadagnini, A., Liu, Q., Hu, B., & Yuan, S. (2022). A computationally efficient method for estimating multi-model process sensitivity index. *Water Resources Research*, *58*(10), e2022WR033263. https://doi.org/10.1029/2022WR033263

Dell'Oca, Riva, M., & Guadagnini, A. (2017). Moment-based metrics for global sensitivity analysis of hydrological systems. *Hydrology and Earth System Sciences*, *21*(12), 6219–6234. https://doi.org/10.5194/hess-21-6219-2017

Devak, M., & Dhanya, C. T. (2017). Sensitivity analysis of hydrological models: Review and way forward. *Journal of Water and Climate Change*, *8*(4), 557–575. https://doi.org/10.2166/wcc.2017.149

Elshall, A. S., Ye, M., & Finkel, M. (2020). Evaluating two multi-model simulation–optimization approaches for managing groundwater contaminant plumes. *Journal of Hydrology*, *590*, 125427. https://doi.org/10.1016/j.jhydrol.2020.125427

Hammond, G. E., Lichtner, P. C., & Mills, R. T. (2014). Evaluating the performance of parallel subsurface simulators: An illustrative example with PFLOTRAN. *Water Resources Research*, *50*(1), 208–228. https://doi.org/10.1002/2012WR013483

Ju, J., Dai, H., Wu, C., Hu, B. X., Ye, M., Chen, X., et al. (2021). Quantifying the uncertainty of the future hydrological impacts of climate change: Comparative analysis of an advanced hierarchical sensitivity in humid and semiarid basins. *Journal of Hydrometeorology*, *22*(3), 601–621. https://doi.org/10.1175/JHM-D-20-0016.1

Knabe, D., Guadagnini, A., Riva, M., & Engelhardt, I. (2021). Uncertainty analysis and identification of key parameters controlling bacteria transport within a riverbank filtration scenario. *Water Resources Research*, *57*(4), e2020WR027911. https://doi.org/10.1029/2020wr027911

Li, M., Di, Z., & Duan, Q. (2021). Effect of sensitivity analysis on parameter optimization: Case study based on streamflow simulations using the SWAT model in China. *Journal of Hydrology*, *603*, 126896. https://doi.org/10.1016/j.jhydrol.2021.126896

Liu, H., Dai, H., Niu, J., Hu, B. X., Gui, D., Qiu, H., et al. (2020). Hierarchical sensitivity analysis for a large-scale process-based hydrological model applied to an Amazonian watershed. *Hydrology and Earth System Sciences*, *24*(10), 4971–4996. https://doi.org/10.5194/hess-24-4971-2020

Mai, J. (2023). Ten strategies towards successful calibration of environmental models. *Journal of Hydrology*, *620*, 129414. https://doi.org/10.1016/j.jhydrol.2023.129414

Markstrom, S. L., Hay, L. E., & Clark, M. P. (2016). Towards simplification of hydrologic modeling: Identification of dominant processes. *Hydrology and Earth System Sciences*, *20*(11), 4655–4671. https://doi.org/10.5194/hess-20-4655-2016

Nossent, J., Elsen, P., & Bauwens, W. (2011). Sobol' sensitivity analysis of a complex environmental model. *Environmental Modelling & Software*, *26*(12), 1515–1525. https://doi.org/10.1016/j.envsoft.2011.08.010

Page, T., Smith, P., Beven, K., Pianosi, F., Sarrazin, F., Almeida, S., et al. (2023). Technical note: The CREDIBLE Uncertainty Estimation (CURE) toolbox: Facilitating the communication of epistemic uncertainty. *Hydrology and Earth System Sciences*, *27*(13), 2523–2534. https://doi.org/10.5194/hess-27-2523-2023

Razavi, S., & Gupta, H. V. (2015). What do we mean by sensitivity analysis? The need for comprehensive characterization of "global" sensitivity in Earth and Environmental systems models. *Water Resources Research*, *51*(5), 3070–3092. https://doi.org/10.1002/2014wr016527

Saltelli, A., Annoni, P., Azzini, I., Campolongo, F., Ratto, M., & Tarantola, S. (2010). Variance based sensitivity analysis of model output. Design and estimator for the total sensitivity index. *Computer Physics Communications*, *181*(2), 259–270. https://doi.org/10.1016/j.cpc.2009.09.018

Schäfer Rodrigues Silva, A., Guthke, A., Höge, M., Cirpka, O. A., & Nowak, W. (2020). Strategies for simplifying reactive transport models: A Bayesian model comparison. *Water Resources Research*, *56*(11), e2020WR028100. https://doi.org/10.1029/2020WR028100

Song, X. M., Zhang, J., Zhan, C., Xuan, Y., Ye, M., & Xu, C. (2015). Global sensitivity analysis in hydrological modeling: Review of concepts, methods, theoretical framework, and applications. *Journal of Hydrology*, *523*, 739–757. https://doi.org/10.1016/j.jhydrol.2015.02.013

Su, Z., & Li, X. (2022). Extraction of key parameters and simplification of sub-system energy models using sensitivity analysis in subway stations. *Energy*, *261*, 125285. https://doi.org/10.1016/j.energy.2022.125285

Wagena, M. B., Bhatt, G., Buell, E., Sommerlot, A. R., Fuka, D. R., & Easton, Z. M. (2019). Quantifying model uncertainty using Bayesian multi-model ensembles. *Environmental Modelling & Software*, *117*, 89–99. https://doi.org/10.1016/j.envsoft.2019.03.013

Walker, A. P., Johnson, A. L., Rogers, A., Anderson, J., Bridges, R. A., Fisher, R. A., et al. (2021). Multi-hypothesis comparison of Farquhar and Collatz photosynthesis models reveals the unexpected influence of empirical assumptions at leaf and global scales. *Global Change Biology*, *27*(4), 804–822. https://doi.org/10.1111/gcb.15366

Walker, A. P., Ye, M., Lu, D., De Kauwe, M. G., Gu, L., Medlyn, B. E., et al. (2018). The multi-assumption architecture and testbed (MAAT v1.0): R code for generating ensembles with dynamic model structure and analysis of epistemic uncertainty from multiple sources. *Geoscientific Model Development*, *11*(8), 3159–3185. https://doi.org/10.5194/gmd-11-3159-2018

Xu, K., Xu, B., Ju, J., Wu, C., Dai, H., & Hu, B. X. (2019). Projection and uncertainty of precipitation extremes in the CMIP5 multimodel ensembles over nine major basins in China. *Atmospheric Research*, *226*, 122–137. https://doi.org/10.1016/j.atmosres.2019.04.018

Yang, J., Liu, Y., Dai, H., Yuan, S., Jiao, T., Wen, Z., & Ye, M. (2024). Development of an integrated global sensitivity analysis strategy for evaluating process sensitivities across single- and multi-models. *Journal of Hydrology*, *643*, 132014. https://doi.org/10.1016/j.jhydrol.2024.132014

Yang, J., & Ye, M. (2022). A new multi-model absolute difference-based sensitivity (MMADS) analysis method to screen non-influential processes under process model and parametric uncertainty. *Journal of Hydrology*, *608*, 127609. https://doi.org/10.1016/j.jhydrol.2022.127609

Yang, J., Ye, M., Chen, X., Dai, H., & Walker, A. P. (2022). Process interactions can change process ranking in a coupled complex system under process model and parametric uncertainty. *Water Resources Research*, *58*(3), e2021WR029812. https://doi.org/10.1029/2021wr029812

Ye, M., Neuman, S. P., & Meyer, P. D. (2004). Maximum likelihood Bayesian averaging of spatial variability models in unsaturated fractured tuff. *Water Resources Research*, *40*(5), W05113. https://doi.org/10.1029/2003wr002557

Ye, M., Pohlmann, K. F., & Chapman, J. B. (2008). Expert elicitation of recharge model probabilities for the Death Valley regional flow system. *Journal of Hydrology*, *354*(1–4), 102–115. https://doi.org/10.1016/j.jhydrol.2008.03.001

Ye, M., Pohlmann, K. F., Chapman, J. B., Pohll, G. M., & Reeves, D. M. (2010). A model-averaging method for assessing groundwater conceptual model uncertainty. *Ground Water*, *48*(5), 716–728. https://doi.org/10.1111/j.1745-6584.2009.00633.x

Yu, Z., Dai, H., Yang, J., Zhu, Y., & Yuan, S. (2024). Global sensitivity analysis with deep learning-based surrogate models for unraveling key parameters and processes governing redox zonation in riparian zone. *Journal of Hydrology*, *638*, 131442. https://doi.org/10.1016/j.jhydrol.2024.131442